Table 1. *Z* scores for L2–4 bone mineral density (BMD) in each allele type (allelic frequency, percentage in the parentheses)

| Allele type | Number of CA repeat | Overall (n = 377; 754 alleles) | ≤10 years (n = 131; 262 alleles) | 10–20 years (n = 144; 288 alleles) | >20 years (n = 102; 204 alleles) |
|---|---|---|---|---|---|
| 1 | 14 | 0.186 ± 0.130 (25.6%) | 0.242 ± 0.149 (28.2%) | 0.155 ± 0.128 (23.6%) | 0.158 ± 0.105 (25.0%) |
| 2 | 16 | 0.203 ± 0.093 (44.4%) | 0.231 ± 0.106 (39.3%) | 0.233 ± 0.150 (47.6%) | 0.124 ± 0.102 (46.6%) |
| 3 | 17 | −0.130 ± 0.171 (7.2%) | −0.028 ± 0.196 (7.6%) | −0.106 ± 0.241 (8.0%) | −0.294 ± 0.246 (5.4%) |
| 4 | 20 | 0.338 ± 0.325 (1.3%) | 0.250 ± 0.271 (1.1%) | 0.031 ± 0.371 (1.4%) | 0.885 ± 0.379 (1.5%) |
| 5 | 22 | −0.282 ± 0.229 (4.6%) | 0.247 ± 0.198 (5.0%) | −0.322 ± 0.223 (3.8%) | −0.868 ± 0.466 (5.4%) |
| 6 | 23 | 0.208 ± 0.250 (2.7%) | 0.308 ± 0.242 (2.7%) | 0.155 ± 0.242 (2.4%) | 0.155 ± 0.247 (2.9%) |
| 7 | 24 | 0.505 ± 0.367 (5.7%) | 0.104 ± 0.110 (6.5%) | 0.444 ± 0.296 (4.9%) | 1.146 ± 0.383 (5.9%) |
| 8 | 25 | 0.337 ± 0.243 (5.2%) | 0.399 ± 0.252 (5.7%) | 0.315 ± 0.267 (5.2%) | 0.288 ± 0.266 (4.4%) |
| 9 | 26 | 0.278 ± 0.367 (2.3%) | 0.034 ± 0.219 (2.7%) | 0.482 ± 0.416 (2.4%) | 0.303 ± 0.678 (1.5%) |
| 10 | 27 | 0.180 ± 0.677 (1.1%) | 0.020 ± 0.338 (1.1%) | 0.288 ± 0.405 (0.7%) | 0.233 ± 0.322 (1.5%) |

Data expressed as mean ± SEM. ≤10 years, women not more than 10 years after menopause; 10–20 years, women more than 10 years and not more than 20 years after menopause; >20 years, women more than 20 years after menopause.

body weight or height differ among allele types in any population (data not shown).

None of the genotypes was associated with bone density in the overall population or in the subpopulation ≤10 years after menopause. Among allele types, types 5 and 7 showed the lowest and the highest mean values of the *Z* score of L2–4 BMD, respectively, in the overall population (Table 1). Type 5 alleles showed lower bone density than other alleles in subpopulations that were 10–20 years ($p = 0.035$) and >20 years after menopause ($p = 0.024$) (**Figure 1**). The type 7 allele was associated with high bone density in women >20 years after menopause ($p = 0.042$) (Figure 1). These results indicate that the human *klotho* gene polymorphism is significantly correlated with bone density in aged women.

### *Association of Klotho Gene Polymorphism With Spondylosis of Postmenopausal Women*

We further investigated the association between the severity of spondylotic change in the lumbar spine expressed as the Kellgren–Lawrence score and the *klotho* gene polymorphism in the 221 postmenopausal women of the 377 for whom lateral X-rays of the lumbar spine were available. The distribution of allelic frequency was similar to that of all 377 women, and was not different among the overall population (n = 221; 442 alleles), the subpopulation equal to or younger than the average age (≤63 years old, n = 119; 238 alleles), and that older than the average age (>63 years old, n = 102; 204 alleles) (**Table 2**). Deviation from Hardy–Weinberg equilibrium also was not significant in any of the subpopulations (all $p > 0.05$). Neither body weight nor height differed among allele types in any population (Table 2).

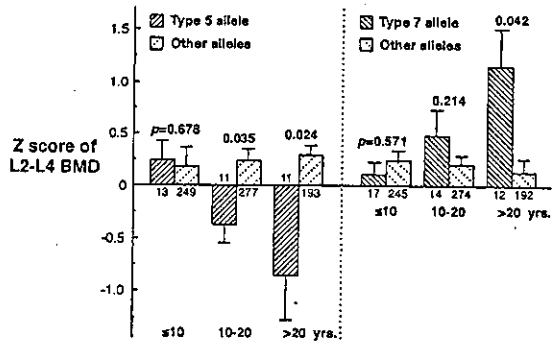


Figure 1. Differences of L2–4 BMD *Z* score between the type 5 allele and other alleles (left); that between type 7 allele and other alleles (right) in subpopulations ≤10 years after menopause (≤10 yrs., n = 131; 262 alleles), >10 years and ≤20 years after menopause (10–20 yrs., n = 144; 288 alleles), and >20 years after menopause (>20 yrs., n = 102; 204 alleles). BMD of the lumbar spine (L2–4, mg/cm$^2$) was measured by dual-energy X-ray absorptiometry and expressed as a *Z* score, which is a deviation from the weight-adjusted average BMD of each age. Data expressed as mean (bars) ± SEM (error bars) for the number of alleles indicated under each bar. Numbers above the bars are the *p* values of the difference in *Z* score. None of the other eight alleles was significantly associated with *Z* score in any subpopulation.

In the association study with the spondylosis score as well, no allele type showed a significant association with the score at either L-4/5 or L-5/S-1 levels in the overall population (Table 2). However, the type 8 allele showed the lowest mean value in all populations (Table 2), and was significantly associated with low spondylosis score at L-4/5 ($p = 0.019$) and L-5/S-1 ($p = 0.048$) levels in the younger population, but not in the older population (**Figure 2**). These results indicate that the microsatellite polymorphism of the human *klotho* gene is correlated with lumbar spondylosis in younger postmenopausal women, which is in contrast to the results of the association with bone density at older ages. In addition, the type 5 or type 7 allele, which was associated with bone density, were not associated with the spondylosis score in any population.

## Discussion

Because we previously reported that the mouse homozygous for a disruption of the *klotho* locus exhibited multiple aging phenotypes, including osteopenia and osteoarthritis,[18,26] the present study investigated the contribution of a microsatellite polymorphism at the human *klotho* locus to bone density and spondylosis of the lumbar spine in Japanese postmenopausal women. Two types of alleles were associated with bone density in the older population, whereas another distinct allele was associated with spondylosis in the younger population, suggesting the contribution of the *klotho* gene to the etiology of osteoporosis and spondylosis in independent ways. These results provide the first evidence that the *klotho* gene may be involved in the etiology of human diseases.

The fact that the association of the *klotho* gene with these disorders is dependent on age cannot be explained by differences in the distribution of allele types among generations, because the allelic frequency was similar in all subpopulations (Tables 1 and 2). It is possible that the lack of change seen in the allelic

Bone Vol. 31, No. 1
July 2002:37–42

Table 2. Kellgren–Lawrence score at L-4/5 and L-5/S-1 levels in each allele type (allelic frequency, percentage in the parentheses)

| | Overall (n = 221; 442 alleles) | | Younger (n = 119; 238 alleles) | | Older (n = 102; 204 alleles) | |
|---|---|---|---|---|---|---|
| Allele type | L-4/5 | L-5/S-1 | L-4/5 | L-5/S-1 | L-4/5 | L-5/S-1 |
| 1 | 2.50 ± 0.12 | 2.34 ± 0.13 (23.5%) | 2.15 ± 0.15 | 1.94 ± 0.16 (23.1%) | 2.87 ± 0.16 | 2.76 ± 0.21 (24.0%) |
| 2 | 2.42 ± 0.08 | 2.33 ± 0.15 (46.2%) | 2.12 ± 0.11 | 1.91 ± 0.12 (46.2%) | 2.74 ± 0.11 | 2.77 ± 0.13 (46.6%) |
| 3 | 2.65 ± 0.19 | 2.74 ± 0.22 (6.8%) | 2.33 ± 0.19 | 2.28 ± 0.24 (7.1%) | 3.02 ± 0.37 | 3.22 ± 0.36 (6.4%) |
| 4 | 2.45 ± 0.22 | 2.25 ± 0.26 (1.8%) | 2.17 ± 0.23 | 1.77 ± 0.67 (1.7%) | 2.75 ± 0.25 | 2.75 ± 0.25 (1.9%) |
| 5 | 2.27 ± 0.21 | 2.26 ± 0.25 (5.0%) | 1.97 ± 0.48 | 1.87 ± 0.33 (5.0%) | 2.60 ± 0.20 | 2.70 ± 0.32 (4.9%) |
| 6 | 2.31 ± 0.19 | 2.25 ± 0.22 (2.7%) | 1.96 ± 0.21 | 1.71 ± 0.20 (2.9%) | 2.70 ± 0.37 | 2.80 ± 0.42 (2.0%) |
| 7 | 2.63 ± 0.21 | 2.54 ± 0.23 (5.4%) | 2.25 ± 0.28 | 2.08 ± 0.34 (5.5%) | 3.02 ± 0.24 | 3.01 ± 0.31 (5.9%) |
| 8 | 2.03 ± 0.21 | 1.99 ± 0.27 (5.7%) | 1.50 ± 0.15 | 1.33 ± 0.26 (5.5%) | 2.58 ± 0.23 | 2.67 ± 0.20 (5.4%) |
| 9 | 2.55 ± 0.36 | 2.53 ± 0.14 (1.6%) | 2.27 ± 0.67 | 2.17 ± 0.11 (1.7%) | 2.87 ± 0.43 | 2.91 ± 0.46 (1.5%) |
| 10 | 2.57 ± 0.15 | 2.47 ± 0.27 (1.3%) | 2.38 ± 0.35 | 2.01 ± 0.39 (1.3%) | 2.79 ± 0.55 | 2.94 ± 0.33 (1.5%) |

Data expressed as mean ± SEM. Younger, women equal to or younger than the average age (≤63 years old); older women older than the average age (>63 years old).

frequency with increasing age might suggest that the *klotho* gene is not associated with longevity, although more detailed study is certainly essential to reach that conclusion.

Osteoporosis and spondylosis are representative age-related skeletal disorders with an etiology that is dependent on both genetic and environment factors. Bone density in women is known to decrease rapidly just after menopause as a result of estrogen withdrawal, and slowly with aging thereafter. The association between the *klotho* locus polymorphism and bone loss in the aged suggests that the *klotho* gene may be involved in the pathophysiology of age-related osteoporosis rather than osteoporosis by menopause. In support of this notion, *klotho*-deficient mice develop low-turnover osteopenia resembling senile osteoporosis.[18] It is further speculated that the product of the *klotho* gene (KL protein) may have an important function in regulating bone density after the influence of estrogen withdrawal at younger ages weakens. An age-related increase in the association between genotypes and bone density was also reported in a study of collagen I α1 polymorphism.[35] These results raise the possibility that the polymorphisms of genes, such as *klotho* and collagen I α1, may be markers for bone loss by aging, rather than markers for the bone loss by menopause and the peak bone density in adolescence. Regarding spondylosis, on the contrary, it is believed that the most important environmental factor is the accumulation of mechanical stress on the spine with aging, and therefore the association of the *klotho* gene might possibly be concealed by this environmental factor at older ages.

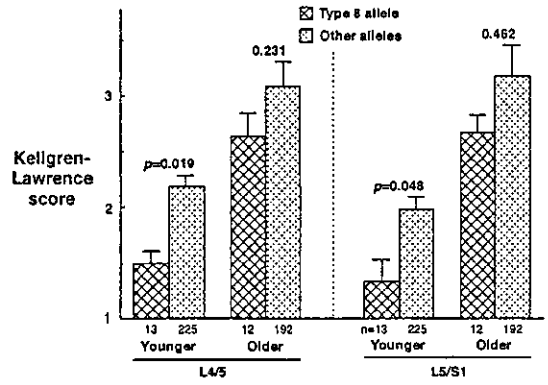


Figure 2. Differences of spondylosis score between the type 8 allele and other alleles in the younger (≤63 years old [average age] n = 119) and the older (>63 years old, n = 102) subpopulations. The severity of spondylotic change at L-4/5 and L-5/S-1 levels was graded on a five point scale (0–4) according to Kellgren–Lawrence scoring on a lateral radiograph of the lumbar spine. Data expressed as mean (bars) ± SEM (error bars) for the number of alleles indicated under each bar. Numbers above the bars are the *p* values of the difference in the Kellgren–Lawrence score between carriers and noncarriers of the allele. None of the other nine alleles was significantly associated with the Kellgren-Lawrence score in any subpopulation.

It is also of interest that the allele associated with spondylosis is different from that associated with bone density. Osteoporosis is a catabolic disorder of bone metabolism whereas osteoarthritis includes an anabolic aspect of subchondral sclerosis and osteophyte formation, implying the existence of some common genetic backgrounds causing these opposite phenotypes. In fact, several epidemiologic studies have shown that bone density in patients with osteoarthritis is greater than that in controls.[4,10,14] However, the facts that the type 8 allele, which was associated with spondylosis, was not associated with bone density, and that the type 5 and 7 alleles, which were associated with bone density, were not associated with spondylosis argue against this possibility, and suggest that the contribution of the *klotho* gene to the development of one disease is, at least in part, independent of the other. A recent report also supports independent genetic backgrounds in these two diseases, although some common environmental factors such as body weight are known to inversely affect them.[10]

This study was the first to demonstrate the involvement of the human *klotho* gene in the etiology of the human age-related diseases of osteoporosis and spondylosis. Considering the rather weak associations in this study, this gene might have a relatively small attributable risk fraction for these polygenic diseases. However, we believe that identification of a possible disease susceptibility/severity gene could lead to a better understanding of the molecular pathogenesis of the disease. The mechanism whereby the change in the *klotho* gene affects bone density and spondylosis remains to be identified. Because this microsatellite region is located outside of the coding region, the polymorphism itself does not directly modulate the production or function of the KL protein. The screening of variations in the coding region of the gene that shows linkage disequilibrium with the associated alleles shown in this study will be necessary to clarify the functional relevance. In fact, our preliminary study has confirmed that single-nucleotide polymorphisms (SNPs) identified in all five exons and the promoter region of the human *klotho* gene show a significant association with bone loss in aged women.[19] However, it should be noted that evaluation of the production or function of the KL protein is difficult at present. This is because the *klotho* gene is expressed in specific tissues

such as kidney and brain, despite the fact that a defect in *klotho* expression causes systemic aging phenotypes. In addition, a means of measuring the serum level of the human KL protein has not yet been established, and the function of the KL protein remains unidentified. Further understanding of the *klotho* gene and the KL protein would help us to recognize their contribution to these age-related disorders.

*Acknowledgments:* This work was supported by grants from the Japanese Ministry of Education, Science, Sports, Culture and Technology (#12137201 and #12307031); the Japan Space Forum; the Uehara Memorial Foundation; Southwestern Medical Foundation at UT Southwestern Medical Center; and the Pew Scholars Program in Biomedical Science.

## References

1. Ala-Kokko, L., Baldwin, C. T., Moskowitz, R. W., and Prockop, D. J. Single base mutation in the type II procollagen gene (COL2A1) as a cause of primary osteoarthritis associated with a mild chondrodysplasia. Proc Natl Acad Sci USA 87:6565–6568; 1990.
2. Battie, M. C., Videman, T., Gibbons, L. E., Fisher, L. D., Manninen, H., and Gill, K. Determinants of lumbar disc degeneration. A study relating lifetime exposures and magnetic resonance imaging findings in identical twins. Spine 20:2601–2612; 1995.
3. Briggs, M. D., Hoffman, S. M., King, L. M., Olsen, A. S., Mohrenweiser, H., Leroy, J. G., Mortier, G. R., Rimoin, D. L., Lachman, R. S., and Gaines, E. S. Pseudoachondroplasia and multiple epiphysial dysplasia due to mutations in the cartilage oligomeric matrix protein gene. Nat Genet 10:330–336; 1995.
4. Burger, H., van Daele, P. L., Odding, E., Valkenburg, H. A., Hofman, A., Grobbee, D. E., Schutte, H. E., Birkenhager, J. C., and Pols, H. A. Association of radiographically evident osteoarthritis with higher bone mineral density and increased bone loss with age. The Rotterdam Study. Arthritis Rheum 39:81–86; 1999.
5. Devoto, M., Shimoya, K., Caminis, J., Ott, J., Tenenhouse, A., Whyte, M. P., Sereda, L., Hall, S., Considine, E., Williams, C. J., Tromp, G., Kuivaniemi, H., Ala-Kokko, L., Prockop, D. J., and Spotila, L. D. First-stage autosomal genome screen in extended pedigrees suggests genes predisposing to low bone mineral density on chromosomes 1p, 2p and 4q. Eur J Hum 6:151–157; 1998.
6. Duncan, E. L., Brown, M. A., Sinsheimer, J., Bell, J., Carr, A. J., Wordsworth, B. P., and Wass, J. A. Suggestive linkage of the parathyroid receptor type 1 to osteoporosis. J Bone Miner Res 14:1993–1999; 1999.
7. Evans, R. A., Marel, G. M., Lancaster, E. K., Kos, S., Evans, M., and Wong, S. Y. P. Bone mass is low in relatives of osteoporotic patients. Ann Intern Med 109:870–873; 1988.
8. Felson, D. T., Couropmitree, N. N., Chaisson, C. E., Hannan, M. T., Zhang, Y., McAlindon, T. E., LaValley, M., Levy, D., and Myers, R. H. Evidence for a Mendelian gene in a segregation analysis of generalized radiographic osteoarthritis: The Framingham Study. Arthritis Rheum 41:1064–1071; 1998.
9. Flicker, L., Hopper, J. L., Rogers, L., Kaymacki, B., Green, R. M., and Wark, J. D. Bone mineral density determinants in elderly women: A twin study. J Bone Miner Res 10:1607–1613; 1995.
10. Fujita, T. Degenerative joint disease: An example of calcium paradox. J Bone Miner Metab 16:195–205; 1998.
11. Garnero, P., Borel, O., Sornay-Rendu, E., Arlot, M. E., and Delmas, P. D. Vitamin D receptor gene polymorphisms are not related to bone turnover, rate of bone loss, and bone mass in postmenopausal women: The OFELY Study. J Bone Miner Res 11:827–834; 1996.
12. Grant, S. F. A., Reid, D. M., Blake, G., Herd, R., Fogelman, I., and Ralston, S. H. Reduced bone density and osteoporotic fracture associated with a polymorphic Sp1 binding site in the collagen type I α1 gene. Nat Genet 14:203–205; 1996.
13. Han, K. O., Moon, I. G., Hwang, C. S., Choi, J. T., Yoon, H. K., Min, H. K., and Han, I. K. Lack of an intronic Sp1 binding-site polymorphism at the collagen type I α1 gene in healthy Korean women. Bone 24:135–137; 1999.
14. Hannan, M. T., Anderson, J. J., Zhang, Y., Levy, D., and Felson, D. T. Bone mineral density and knee osteoarthritis in elderly men and women. The Framingham Study. Arthritis Rheum 36:1671–1680; 1993.
15. Hecht, J. T., Nelson, L. D., Crowder, E., Wang, Y., Elder, F. F., Harrison, W. R., Francomano, C. A., Prange, C. K., Lennon, G. G., and Deere, M. Mutations in exon 17B of cartilage oligomeric matrix protein (COMP) cause pseudoachondroplasia. Nat Genet 10:325–329; 1995.
16. Hirsch, R., Lethbridge-Cejku, M., Hanson, R., Scott, W. W. Jr., Reichle, R., Plato, C. C., Tobin, J. D., and Hochberg, M. C. Familial aggregation of osteoarthritis: Data from the Baltimore Longitudinal Study on Aging. Arthritis Rheum 41:1227–1232; 1998.
17. Hustmyer, F. G., Peacock, M., Hui, S., Johnston, C. C., and Christian, J. Bone mineral density in relation to polymorphism at the vitamin D receptor gene locus. J Clin Invest 94:2130–2134; 1994.
18. Kawaguchi, H., Manabe, N., Miyaura, C., Chikuda, H., Nakamura, K., and Kuro-o, M. Independent impairment of osteoblast and osteoclast differentiation in *klotho* mouse exhibiting low-turnover osteopenia. J Clin Invest 104:229–237; 1999.
19. Kawano, K., Ogata, N., Suzuki, T., Yoshida, H., Hosoi, T., Orimo, H., Inoue, S., Koshizuka, M., Kuro-o, M., Nakamura, K., and Kawaguchi, H. Identification of coding region single-nucleotide polymorphisms (cSNPs) in the human *klotho* gene and their association with bone density in postmenopausal women. J Bone Miner Res 15(Suppl. 1):S214; 2000.
20. Keen, R. W., Hart, D. J., Lanchbury, J. S., and Spector, T. D. Association of early osteoarthritis of the knee with a Taq I polymorphism of the vitamin D receptor gene. Arthritis Rheum 40:1444–1449; 1997.
21. Kellgren, J. H., Lawrence, J. S., and Bier, F. Genetic factors in generalised osteoarthritis. Ann Rheum Dis 22:237–255; 1963.
22. Knowlton, R. G., Katzenstein, P. L., Moskowitz, R. W., Weaver, E. J., Malemud, C. J., Pathria, M. N., Jimenez, S. A., and Prockop, D. J. Genetic linkage of a polymorphism in the type II procollagen gene (COL2A1) to primary osteoarthritis associated with mild chondrodysplasia. N Engl J Med 322:526–530; 1990.
23. Kobayashi, S., Inoue, S., Hosoi, T., Ouchi, Y., Shiraki, M., and Orimo, H. Association of bone mineral density with polymorphism of the estrogen receptor gene. J Bone Miner Res 11:306–311; 1996.
24. Koller, D. L., Econs, M. J., Morin, P. A., Christian, J. C., Hui, S. L., Parry, P., Curran, M. E., Rodriguez, L. A., Conneally, P. M., Joslyn, G., Peacock, M., Johnston, C. C., and Foroud, T. Genome screen for QTLs contributing to normal variation in bone mineral density and osteoporosis. J Clin Endocrinol Metab 85:3116–3120; 2000.
25. Krall, E. A. and Dawson-Hughes, B. Heritability and life-style determinants of bone mineral density. J Bone Miner Res 8:1–9; 1993.
26. Kuro-o, M., Matsumura, Y., Aizawa, H., Kawaguchi, H., Suga, T., Utsugi, T., Ohyama, Y., Kurabayashi, M., Kaname, T., Kume, E., Iwasaki, H., Iida, A., Shiraki-Iida, T., Nishikawa, S., Nagai, R., and Nabeshima, Y. Mutation of the mouse *klotho* gene leads to a syndrome resembling aging. Nature 390:45–51; 1997.
27. Matsumura, Y., Aizawa, H., Shiraki-Iida, T., Nagai, R., Kuro-o, M., and Nabeshima, Y. Identification of the human *klotho* gene and its two transcripts encoding membrane and secreted *klotho* protein. Biochem Biophys Res Commun 242:626–630; 1998.
28. Morrison, N. A., Qi, J. C., Tokita, A., Kelly, P. J., Crofts, L., Nguyen, T. V., Sambrook, P. N., and Eisman, J. A. Prediction of bone density by vitamin D receptor alleles. Nature 367:284–287; 1994.
29. Niu, T., Chen, C., Cordell, H., Yang, J., Wang, B., Wang, Z., Fang, Z., Schork, N. J., Rosen, C. J., and Xu, X. A genome-wide scan for loci linked to forearm bone mineral density. Hum Genet 104:226–233; 1999.
30. Pocock, N. A., Eisman, J. A., Hopper, J. L., Yeates, M. G., Sambrook, P. N., and Eberl, S. Genetic determinants of bone mass in adults: A twin study. J Clin Invest 80:706–710; 1987.
31. Sambrook, P. N., MacGregor, A. J., and Spector, T. D. Genetic influences on cervical and lumbar disc degeneration: A magnetic resonance imaging study in twins. Arthritis Rheum 42:366–372; 1999.
32. Smith, D. M., Nance, W. E., Kang, K. W., Christian, J. C., and Johnston, C. C. Jr. Genetic factors in determining bone mass. J Clin Invest 52:2800–2808; 1973.
33. Spector, T. D., Cicuttini, F., Baker, J., Loughlin, J., and Hart, D. Genetic influences on osteoarthritis in women: A twin study. Br Med J 312:940–943; 1996.
34. Uitterlinden, A. G., Burger, H., Huang, Q. J., Odding, E., Duijn, C. M., and Hofman, A. Vitamin D receptor genotype is associated with radiographic osteoarthritis at the knee. J Clin Invest 100:259–263; 1997.
35. Uitterlinden, A. G., Burger, H., Huang, Q., Yue, F., McGuigan, F. E., Grant, S. F., Hofman, A., van Leeuwen, J. P., Pols, H. A., and Ralston, S. H. Relation of alleles of the collagen type Iα1 gene to bone density and the risk of osteoporotic fractures in postmenopausal women. N Engl J Med 338:1016–1021; 1998.

36. Vandevyver, C., Vanhoof, J., Declerck, K., Stinissen, P., Vandervorst, C., Michiels, L., Cassiman, J. J., Boonen, S., Raus, J., and Geusens, P. Lack of association between estrogen receptor genotypes and bone mineral density, fracture history, or muscle strength in elderly women. J Bone Miner Res 14:1576–1582; 1999.
37. Vikkula, M., Mariman, E. C., Lui, V. C., Zhidkova, N. I., Tiller, G. E., Goldring, M. B., van Beersum, S. E., de Waal Malefijt, M. C., van den Hoogen, F. H., and Ropers, H. H. Autosomal dominant and recessive osteochondrodysplasias associated with the COL11A2 locus. Cell 80:431–437; 1995.
38. Yamada, Y., Okuizumi, H., Miyauchi, A., Takagi, Y., Ikeda, K., and Harada, A. Association of transforming growth factor beta1 genotype with spinal osteophytosis in Japanese women. Arthritis Rheum 43:452–460; 2000.
39. Young, D., Hopper, J. L., Nowson, C. A., Green, R. M., Sherwin, A. J., Kaymakci, B., Smid, M., Guest, C. S., Larkins, R. G., and Wark, J. D. Determinants of bone mass in 10 to 26 year old females: A twin study. J Bone Miner Res 10:558–567; 1995.

*Date Received:* July 24, 2001
*Date Revised:* January 31, 2002
*Date Accepted:* February 19, 2002

JCB Article

# Insulin receptor substrate-2 maintains predominance of anabolic function over catabolic function of osteoblasts

Toru Akune,[1] Naoshi Ogata,[1] Kazuto Hoshi,[1] Naoto Kubota,[2] Yasuo Terauchi,[2] Kazuyuki Tobe,[2] Hideko Takagi,[3] Yoshiaki Azuma,[3] Takashi Kadowaki,[2] Kozo Nakamura,[1] and Hiroshi Kawaguchi[1]

[1]Department of Orthopaedic Surgery and [2]Department of Metabolic Diseases, University of Tokyo, Tokyo 113-8655, Japan
[3]Teijin Co. Ltd., Tokyo 191-8512, Japan

Insulin receptor substrates (IRS-1 and IRS-2) are essential for intracellular signaling by insulin and insulin-like growth factor-I (IGF-I), anabolic regulators of bone metabolism. Although mice lacking the *IRS-2* gene (*IRS-2*$^{-/-}$ mice) developed normally, they exhibited osteopenia with decreased bone formation and increased bone resorption. Cultured *IRS-2*$^{-/-}$ osteoblasts showed reduced differentiation and matrix synthesis compared with wild-type osteoblasts. However, they showed increased receptor activator of nuclear factor κB ligand (RANKL) expression and osteoclastogenesis in the coculture with bone marrow cells, which were restored by reintroduction of IRS-2 using an adenovirus vector. Although IRS-2 was expressed and phosphorylated by insulin and IGF-I in both osteoblasts and osteoclastic cells, cultures in the absence of osteoblasts revealed that intrinsic IRS-2 signaling in osteoclastic cells was not important for their differentiation, function, or survival. It is concluded that IRS-2 deficiency in osteoblasts causes osteopenia through impaired anabolic function and enhanced supporting ability of osteoclastogenesis. We propose that IRS-2 is needed to maintain the predominance of bone formation over bone resorption, whereas IRS-1 maintains bone turnover, as we previously reported; the integration of these two signalings causes a potent bone anabolic action by insulin and IGF-I.

## Introduction

Bone is continually being remodelled according to physiological circumstances through bone formation by osteoblasts and resorption by osteoclasts. These two processes are closely coupled, and bone mass is maintained without change by their balance in healthy adults. A rupture of the balance causing a predominance of bone resorption over bone formation results in bone loss such as that seen in osteoporosis. Among many systemic and local factors involved in the regulation of bone metabolism, insulin and insulin-like growth factor-I (IGF-I)* are known to play important anabolic roles (Canalis, 1993; Thomas et al., 1997). Patients with insulin deficiency as exemplified by type 1 diabetes are associated with osteoporosis (Krakauer et al., 1997; Piepkorn et al., 1997); those with Laron syndrome caused by IGF-I deficiency also exhibit this condition (Laron et al., 1999). A reduction in IGF-I is also implicated as an important factor in the etiology of involutional osteoporosis, especially of age-related bone loss (Nicolas et al., 1994; Rosen, 1994; Reed et al., 1995; Canalis, 1997). However, the cellular and molecular mechanism underlying bone loss due to the deficiency of insulin and IGF-I signalings has not yet been clarified.

Insulin and IGF-I initiate cellular responses by binding to distinct cell surface receptor tyrosine kinases that regulate a variety of signaling pathways controlling metabolism, growth, and survival. Insulin receptor substrates (IRSs) are essential substrates of both of the receptor tyrosine kinases, which integrate the pleiotropic effects of insulin, IGF-I, and other cytokines on cellular function (Kadowaki et al., 1996;

Address correspondence to Hiroshi Kawaguchi, M.D., Ph.D, Department of Orthopaedic Surgery, Faculty of Medicine, University of Tokyo, Hongo 7-3-1, Bunkyo-ku, Tokyo 113-8655, Japan. Tel.: 81-33815-5411, ext. 30473 or 33376. Fax: 81-33818-4082.
E-mail: kawaguchi-ort@h.u-tokyo.ac.jp

*Abbreviations used in this paper: ALP, alkaline phosphatase; BMD, bone mineral density; BMP-2, bone morphogenetic protein 2; Id-1, inhibitor of differentiation-1; IGF-I, insulin-like growth factor-I; IL, interleukin; IRS, insulin receptor substrate; Lrp5, LDL receptor–related protein 5; M-BMMϕ, M-CSF–dependent bone marrow macrophage; M-CSF, macrophage colony-stimulating factor; MMP-13, matrix metalloproteinase-13; MOI, multiplicity of infection; $PGE_2$, prostaglandin $E_2$; PI3, phosphatidylinositol 3; RANKL, receptor activator of nuclear factor κB ligand; TRAP, tartrate-resistant acid phosphatase; WT, wild type.

Key words: insulin-like growth factor-I; osteoclast; osteoporosis; diabetes mellitus; cytokine


The Journal of Cell Biology, Volume 159, Number 1, October 14, 2002 147–156
http://www.jcb.org/cgi/doi/10.1083/jcb.200204046

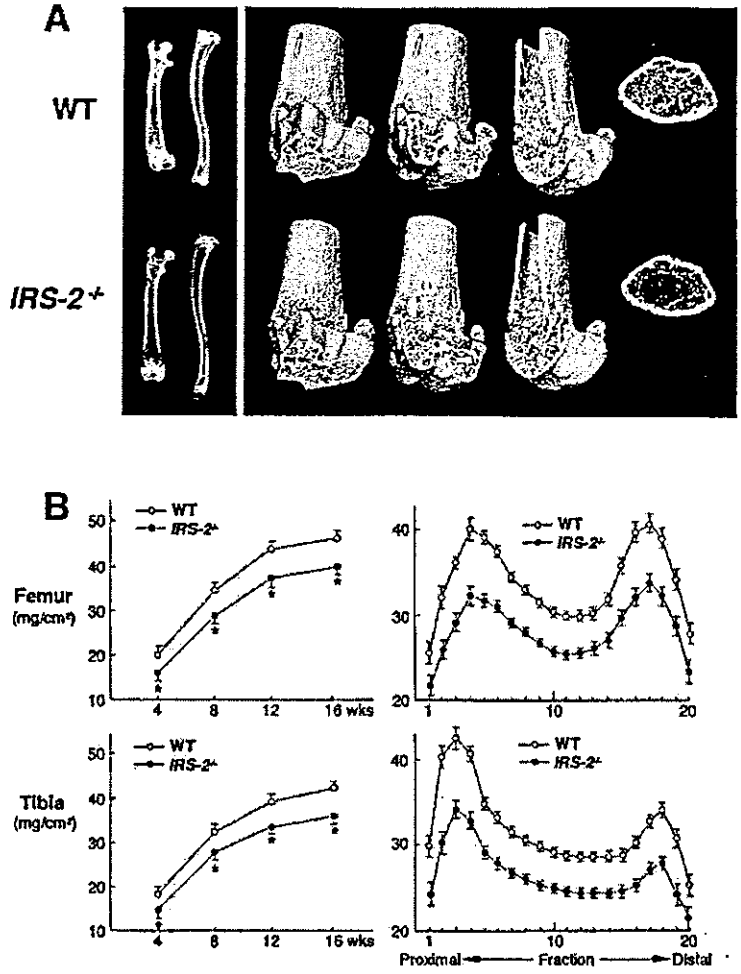


Figure 1. ***IRS-2*$^{-/-}$ mice showed osteopenia both in trabecular and cortex bones.** (A) Plain X-ray images of femora and tibiae (left) and three-dimensional CT images of distal femora (right) of representative WT and *IRS-2*$^{-/-}$ littermates (8 wk old). (B) BMD of the femora and tibiae of WT and *IRS-2*$^{-/-}$ littermates. (B, left) BMD of the whole femora and tibiae at 4, 8, 12, and 16 wk of age. *, significantly different from WT mice; $P < 0.05$. (B, right) BMD of each of 20 equal longitudinal divisions of the femora and tibiae of 8-wk-old mice. Data are expressed as means (symbols) ± SEMs (error bars) for 12 bones/group for WT and *IRS-2*$^{-/-}$ mice.

White, 1998; Burks and White, 2001). The mammalian IRS family contains at least four members, ubiquitous IRS-1 and IRS-2, adipose tissue-predominant IRS-3 (Lavan et al., 1997b), and IRS-4, which is expressed in thymus, brain, and kidney (Lavan et al., 1997a). In bone cells, IRS-1 and IRS-2 are expressed, and we previously reported that IRS-1 in osteoblasts is indispensable for maintaining bone turnover because *IRS-1*$^{-/-}$ mice showed osteopenia with a low bone turnover in which both bone formation and resorption were decreased (Ogata et al., 2000).

IRS-1 and IRS-2 signalings are reported to have distinct biological roles and to be differentially expressed in a variety of cells. Regarding glucose homeostasis, IRS-1 plays an important role in the metabolic actions of insulin and IGF-I mainly in skeletal muscle and adipose tissue, whereas IRS-2 does so in the liver (Yamauchi et al., 1996; Bruning et al., 1997). Most hemopoietic cells express IRS-2 but not IRS-1 (Sun et al., 1997), and in bone cells as well, IRS-1 expression was limited to osteoblastic cells, whereas IRS-2 was expressed in both osteoblastic and osteoclastic cells (Ogata et al., 2000). In addition, IRS-2 is known as a signaling molecule of interleukin (IL)-4 and IL-13, cytokines with inhibitory effects on osteoclastogenesis (Wang et al., 1998; Scopes et al., 2001; Wurster et al., 2002). Hence, there is a possibility that IRS-2 has a different function in the regulation of bone metabolism from that of IRS-1, especially in the catabolic phase by osteoclastic cells.

This study analyzed the bones of mice lacking the *IRS-2* gene (*IRS-2*$^{-/-}$ mice), which we generated by homologous recombination (Kubota et al., 2000). *IRS-2*$^{-/-}$ mice were normal in appearance with a body size similar to wild-type (WT) mice and showed no abnormalities in major organs such as brain, heart, liver, spleen, or kidney, except that their general adiposity was slightly increased and females were infertile (Withers et al., 1998; Burks et al., 2000; Kubota et al., 2000; Tobe et al., 2001). These phenotypes were also different from *IRS-1*$^{-/-}$ mice whose growth was significantly retarded and in which group both males and females were fertile (Araki et al., 1994; Tamemoto et al., 1994). Furthermore, *IRS-2*$^{-/-}$ mice displayed type 2 diabetes with peripheral insulin resistance and pancreatic β cell dysfunction characterized by reduction in β cell mass, whereas *IRS-1*$^{-/-}$ mice did not develop diabetes due to an enhanced β cell mass that compensated for the peripheral insulin resistance.

In this study, we first found osteopenia in *IRS-2*$^{-/-}$ mice, and sought to determine the cellular and molecular mechanism underlying the abnormality of bone metabolism using in vivo morphological analyses and in vitro cell culture systems.

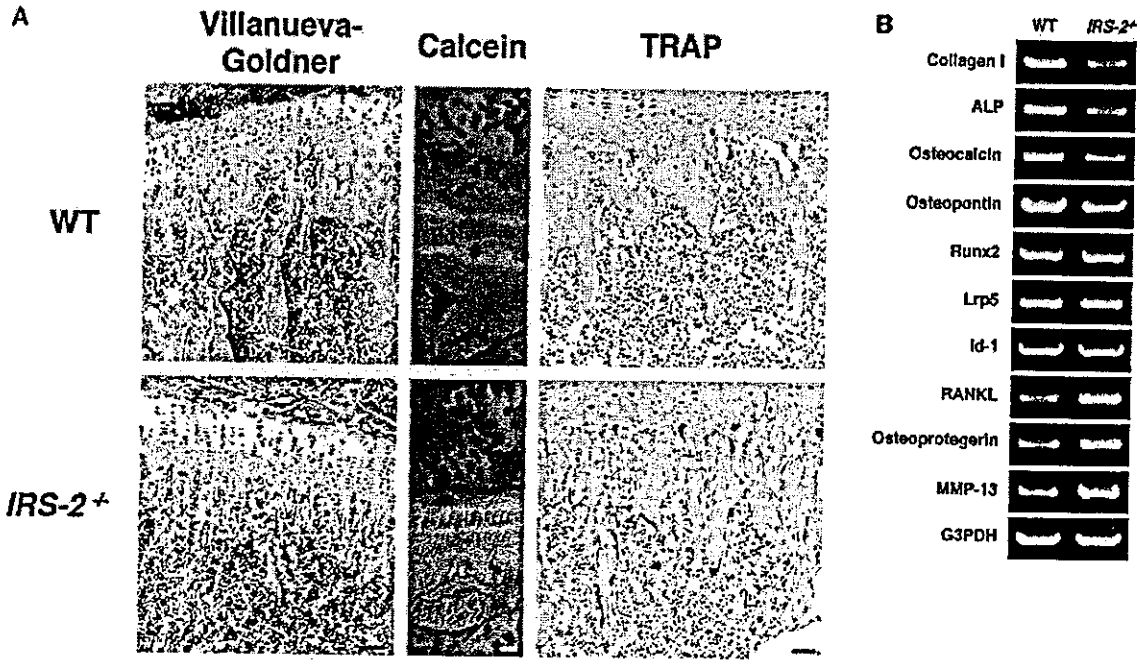


Figure 2. ***IRS-2*$^{-/-}$ bone showed an uncoupling of decreased bone formation and increased bone resorption in vivo.** (A) Histological features at proximal tibiae of WT and *IRS-2*$^{-/-}$ littermates (8 wk old). In Villanueva-Goldner staining (left), mineralized bone is stained green and unmineralized osteoid red. Bar, 50 μm. In calcein double labeling (middle), mineralization front is stained as a green line. Bar, 10 μm. In TRAP staining, TRAP-positive osteoclasts are stained red. Bar, 50 μm. Data of histomorphometric parameters are shown in Table I. (B) Expression of matrix proteins (type I collagen, ALP, osteocalcin, and osteopontin) and key molecules for differentiations of osteoblasts (Runx2, Lrp5, and Id-1) and osteoclasts (RANKL, osteoprotegerin, and MMP-13) in long bones of WT and *IRS-2*$^{-/-}$ littermates (5 wk old) by semiquantitative RT-PCR.

## Results

### *IRS-2*$^{-/-}$ mice showed osteopenia with an uncoupling of decreased bone formation and increased bone resorption

Because the lengths of femora and tibiae did not differ between WT and *IRS-2*$^{-/-}$ littermates at 8 wk of age (Fig. 1 A), IRS-2 was suggested not to be involved in the regulation of skeletal growth. However, *IRS-2*$^{-/-}$ mice showed osteopenia in these long bones by X-ray and three-dimensional CT analyses (Fig. 1 A). This was also found in vertebral bodies (unpublished data). Bone mineral density (BMD) of these bones was decreased by ~10–15% in *IRS-2*$^{-/-}$ mice at 4, 8, 12, and 16 wk of age compared with their WT littermates (Fig. 1 B, left). To determine the distribution of BMD of long bones at 8 wk, the femora and tibiae were analyzed by dividing them longitudinally into 20 equal regions (Fig. 1 B, right). BMD of each fraction was similarly decreased in all fractions of *IRS-2*$^{-/-}$ bones, suggesting that both trabecular and cortex bones were similarly affected by IRS-2 deficiency.

Histological features of the proximal tibiae of 8-wk-old *IRS-2*$^{-/-}$ mice displayed a decrease in the trabecular bone volume (Fig. 2 A, left). Calcein double labeling showed that the width between the two stained labels was narrower in *IRS-2*$^{-/-}$ (Fig. 2 A, middle); however, the number of tartrate-resistant acid phosphatase (TRAP)–positive osteoclasts was higher in *IRS-2*$^{-/-}$ than in WT littermates (Fig. 2 A, right). Histomorphometric measurements revealed that bone volume (BV/TV) was ~30% decreased, and parameters for bone resorption (Oc.N/B.Pm, Oc.S/BS, and ES/BS) were 70–80% increased in *IRS-2*$^{-/-}$ compared with WT littermates (Table I). Regarding bone formation parameters, osteoblast number (Ob.S/BS) was slightly, although not significantly, increased in *IRS-2*$^{-/-}$ bones. However, mineral apposition rate (MAR), reflecting the ability of an individual osteoblast to form bone, was ~50% decreased, and, consequently, bone formation rate (BFR/BS) was significantly lower in *IRS-2*$^{-/-}$ compared with WT littermates. Taking these in vivo observations together, *IRS-2*$^{-/-}$ mice exhibited osteopenia with increased osteoclastic bone resorption and decreased osteoblastic bone formation, suggesting that the two actions were not coupled. The thickness of the growth plate at the proximal tibiae was not different between *IRS-2*$^{-/-}$ and WT littermates (70.8 ± 8.9 and 76.9 ± 10.8 μm, mean ± SEM of eight mice each, respectively), indicating that IRS-2 signaling is not important for chondrocytes.

To further investigate the regulation of expression of genes related to bone metabolism by IRS-2 deficiency, we compared mRNA levels of matrix proteins and key molecules for osteoblast and osteoclast differentiations in long bones between *IRS-2*$^{-/-}$ and WT littermates (Fig. 2 B). Expression of matrix proteins such as type I collagen, alkaline phosphatase (ALP), osteocalcin, and osteopontin was decreased in *IRS-2*$^{-/-}$ bones, which was consistent with the histomorphometric data showing reduced bone formation. However, expression of the putative central determinants of major pathways for osteoblast differentiation, i.e., Runx2 (Karsenty, 2001), LDL receptor–related protein 5 (Lrp5) (Patel and Karsenty, 2002), and inhibitor of differentiation-1 (Id-1) (Ogata et al., 1993), was not different between

Table I. **Histomorphometry of trabecular and cortex bones of tibiae**

| | Trabecular | | | | | | | Cortex |
|---|---|---|---|---|---|---|---|---|
| | BV/TV | Ob.S/BS | MAR | BFR | Oc.N/B.Pm | Oc.S/BS | ES/BS | C.Th |
| | % | % | μm/d | mm²/cm²/y | /100 mm | % | % | $\times 10^{-1}$ mm |
| WT | 9.86 ± 0.74 | 8.93 ± 1.83 | 2.03 ± 0.25 | 4.06 ± 0.44 | 136.19 ± 19.26 | 4.92 ± 0.68 | 5.22 ± 0.89 | 2.59 ± 0.13 |
| *IRS-2*$^{-/-}$ | 6.95 ± 0.63[b] | 13.71 ± 2.51 | 1.08 ± 0.16[b] | 2.71 ± 0.38[a] | 244.27 ± 22.96[b] | 8.71 ± 1.03[b] | 9.14 ± 0.91[b] | 2.18 ± 0.12[a] |

Parameters for the trabecular bone were measured in an area 1.2 mm in length from 0.5 mm below the growth plate at the proximal metaphysis of the tibiae in Villanueva-Goldner and calcein double-labeled sections. Parameters for the cortex bone were measured at the midpoint of the tibiae. Data are expressed as means ± SEMs for eight bones/group for WT and *IRS-2*$^{-/-}$ mice. BV/TV, trabecular bone volume expressed as a percentage of total tissue volume; Ob.S/BS, percentage of bone surface covered by cuboidal osteoblasts; MAR, mineral apposition rate; BFR, bone formation rate expressed by MAR × percentage of bone surface exhibiting double labels plus one half single labels; Oc.N/B.Pm, number of mature osteoclasts in 10 cm of bone perimeter; Oc.S/BS, percentage of bone surface covered by mature osteoclasts; ES/BS, percentage of eroded surface; C.Th, cortex thickness.
[a]Significantly different from WT mice; $P < 0.05$.
[b]Significantly different from WT mice; $P < 0.01$.

WT and *IRS-2*$^{-/-}$ bones, implying an independent signaling pathway of IRS-2 in osteoblasts. Positive regulatory molecules of bone resorption, such as receptor activator of nuclear factor κB ligand (RANKL) (Suda et al., 1999) and matrix metalloproteinase-13 (MMP-13) (Uchida et al., 2000), were increased in *IRS-2*$^{-/-}$ bones, which was also consistent with the histomorphometric data showing enhanced bone resorption. The stimulation of expression of osteoprotegerin, a decoy receptor of RANKL and a negative regulator of osteoclastic bone resorption, observed in *IRS-2*$^{-/-}$ bones might possibly be due to a compensative response to enhanced bone resorption, as is reported in postmenopausal women (Yano et al., 1999).

The serum insulin level was significantly higher in *IRS-2*$^{-/-}$ mice than in WT littermates both before (0.91 ± 0.08 vs. 0.25 ± 0.06 ng/ml at 8 wk and 1.23 ± 0.16 vs. 0.44 ± 0.07 ng/ml at 16 wk, mean ± SEM of five mice each) and after (1.64 ± 0.09 vs. 0.54 ± 0.04 ng/ml at 8 wk and 2.33 ± 0.39 vs. 0.67 ± 0.12 ng/ml at 16 wk) glucose load, as reported previously (Kubota et al., 2000). Serum IGF-I level was similar between *IRS-2*$^{-/-}$ and WT littermates (134.21 ± 11.42 vs. 132.14 ± 10.65 ng/ml, respectively) at 8 wk, with no significant change at 16 wk in either type of mice.

## IRS-2 was expressed and phosphorylated in both osteoblasts and osteoclastic cells of WT mice

Because IRS-1 and IRS-2 are reported to be differentially expressed in a variety of cells and tissues having different biological roles, we compared their expression patterns in primary calvarial osteoblasts. Macrophage colony-stimulating factor (M-CSF)–dependent bone marrow macrophages (M-BMMϕ) as osteoclast precursors and mature osteoclasts isolated from the coculture of osteoblasts and bone marrow cells were taken from WT and *IRS-2*$^{-/-}$ littermates. Both IRS-1 and IRS-2 were expressed in WT osteoblasts, whereas in *IRS-2*$^{-/-}$ osteoblasts, only IRS-1 was expressed with no compensatory increase for IRS-2 deficiency (Fig. 3 A). Re-



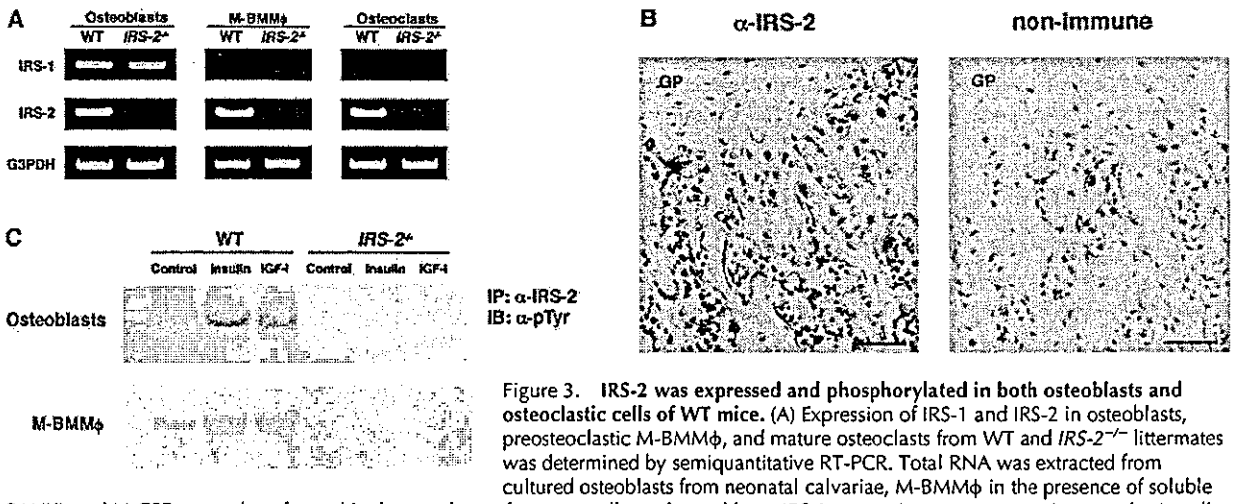


Figure 3. **IRS-2 was expressed and phosphorylated in both osteoblasts and osteoclastic cells of WT mice.** (A) Expression of IRS-1 and IRS-2 in osteoblasts, preosteoclastic M-BMMϕ, and mature osteoclasts from WT and *IRS-2*$^{-/-}$ littermates was determined by semiquantitative RT-PCR. Total RNA was extracted from cultured osteoblasts from neonatal calvariae, M-BMMϕ in the presence of soluble RANKL and M-CSF, osteoclasts formed in the coculture of marrow cells, and osteoblasts. IRS-1 expression was not seen in osteoclastic cells even when the amount of template cDNA or the number of amplification cycles was increased. (B) Immunohistochemical stainings with an anti–IRS-2 antibody (α-IRS-2, left) and a nonimmune serum as a control (right) in the proximal tibial metaphysis of 4-wk-old WT mice. Positive and specific stainings shown in brown are seen in both osteoblasts on the bone surface and osteoclasts (arrowheads). GP, growth plate. Bar, 50 μm. (C) Phosphorylation of IRS-2 in osteoblasts and M-BMMϕ from WT and *IRS-2*$^{-/-}$ mice in the control culture and cultures stimulated by insulin or IGF-I. Osteoblasts and M-BMMϕ from WT and *IRS-2*$^{-/-}$ littermates were cultured with and without insulin or IGF-I for 2 min, and extracted cellular proteins were immunoprecipitated with an anti–IRS-2 antibody (α-IRS-2). After being subjected to SDS-PAGE, they were immunoblotted with an antiphosphotyrosine antibody (α-pTyr).

garding cells of osteoclastic lineage, IRS-1 expression was not detected either in M-BMMϕ or mature osteoclasts, and only IRS-2 was expressed in both of these cells from WT mice (Fig. 3 A).

Immunohistochemical analysis confirmed the expression pattern of IRS-2 in the proximal tibial metaphysis of 4-wk-old WT mice (Fig. 3 B). It was localized in both osteoblasts and osteoclasts on the bone surface. This staining was specific to IRS-2 because neither of these cells was stained with a nonimmune serum.

Fig. 3 C shows the immunoblotting with an antiphosphotyrosine antibody for the extracts immunoprecipitated with an anti–IRS-2 antibody in cultured osteoblasts and M-BMMϕ. IRS-2 protein was confirmed to be expressed in both cells from WT mice, but not in those from *IRS-2*$^{-/-}$ mice. This protein was phosphorylated by insulin and IGF-I potently in osteoblasts whereas slightly in M-BMMϕ.

## Differentiation and anabolic function of osteoblasts were impaired by IRS-2 deficiency

To learn the cellular mechanism underlying the abnormalities in the bone of *IRS-2*$^{-/-}$ mice, we first compared the proliferation, differentiation, and matrix synthesis of cultured osteoblasts from WT and *IRS-2*$^{-/-}$ calvariae. Cell proliferation determined by [$^3$H]thymidine uptake was similarly seen between WT and *IRS-2*$^{-/-}$ cultures (Fig. 4 A); however, cell differentiation determined by ALP activity was significantly decreased in *IRS-2*$^{-/-}$ not only in the control culture, but also in the culture with insulin or IGF-I (Fig. 4 B). Neither potent stimulation of cell proliferation by FGF-2 nor that of cell differentiation by bone morphogenetic protein 2 (BMP-2) was decreased by IRS-2 deficiency. Alizarin red S staining also showed decreased calcified matrix synthesis by *IRS-2*$^{-/-}$ osteoblasts in cultures with and without insulin/IGF-I (Fig. 4 C). Here again, similar potent stimulation by BMP-2 was seen in WT and *IRS-2*$^{-/-}$ osteoblast cultures, suggesting that IRS-2 and BMP-2 systems are independent in osteoblasts. These results indicate that osteoblast differentiation and anabolic function, but not its proliferation, were impaired by IRS-2 deficiency.

We further compared the mRNA levels of Runx2, Lrp5, and Id-1, in addition to the matrix proteins type I collagen, ALP, osteocalcin, and osteopontin in cultured osteoblasts (Fig. 4 D). The results were similar to those seen in vivo: matrix proteins were decreased, but none of Runx2, Lrp5, and Id-1 was affected by IRS-2 deficiency. This again indicates that IRS-2 does not directly impact these major pathways for osteoblast differentiation.

## Osteoclastogenesis and RANKL expression in osteoblasts were enhanced by IRS-2 deficiency

Osteoclasts are known to be derived from hemopoietic cells and to require the cell–cell interaction with osteoblasts/stromal cells for differentiation. To investigate osteoclast formation, we measured the number of TRAP-positive multinucleated osteoclasts formed in the coculture system of osteoblasts and bone marrow cells. Osteoclastogenesis in the coculture induced by the bone resorptive factors prostaglandin $E_2$ ($PGE_2$), IL-11, and $1,25(OH)_2D_3$ was more increased when both cells were derived from *IRS-2*$^{-/-}$ mice than when both cells were derived from WT mice (Fig. 5 A, top). IGF-I slightly, but not significantly, induced osteoclastogenesis in both WT and *IRS-2*$^{-/-}$ cocultures. IL-4 and IL-13 inhibited $1,25(OH)_2D_3$-induced osteoclastogenesis in the WT coculture. Although IRS-2 is known as a signaling molecule of IL-4 and IL-13, neither of the inhibitory actions was different between WT and *IRS-2*$^{-/-}$ cocultures. These results indicate that IRS-2 signaling acts inhibitorily on the induction of osteoclastogenesis by $PGE_2$, IL-11, and $1,25(OH)_2D_3$, but is not related to its inhibition by IL-4 or IL-13. The results were reproducible when spleen cells were used instead of bone marrow cells as a source of hemopoietic cells (unpublished data). Because RANKL is known to be a key membrane-associated molecule expressed on osteoblasts/stromal cells inducing osteoclastogenesis (Suda et al., 1999), we examined the regulation of RANKL expression in osteoblasts from WT and *IRS-2*$^{-/-}$ mice by these factors (Fig. 5 A, bottom). The regulation of RANKL expression showed

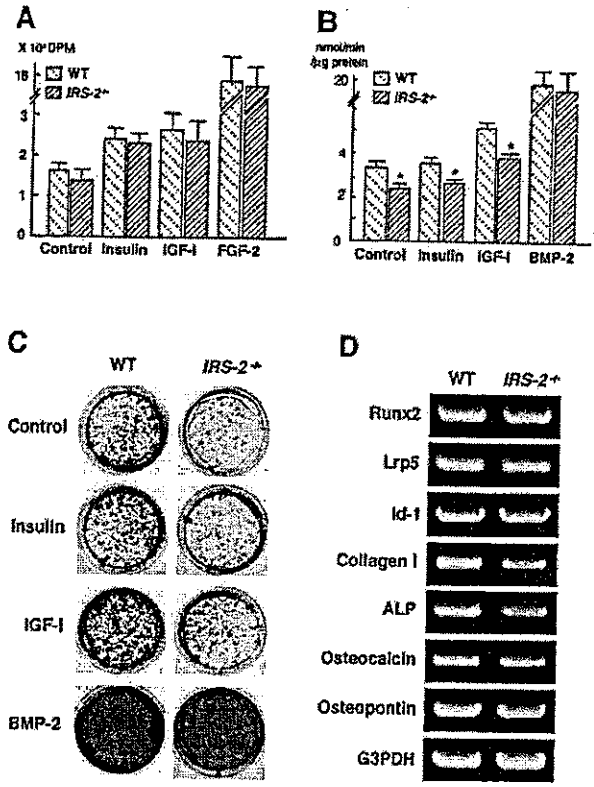


Figure 4. **Osteoblast differentiation and matrix synthesis, but not proliferation, were impaired by IRS-2 deficiency.** (A) Proliferation determined by [$^3$H]TdR incorporation into osteoblasts from WT and *IRS-2*$^{-/-}$ calvariae cultured with and without insulin, IGF-I, or FGF-2 for 24 h. (B) ALP activity of osteoblasts from WT or *IRS-2*$^{-/-}$ calvariae cultured with and without insulin, IGF-I, or BMP-2 for 14 d. For A and B, data are expressed as means (bars) ± SEMs (error bars) for eight wells/group. *, significant decrease by IRS-2 deficiency; $P < 0.05$. (C) Calcified matrix synthesis determined by Alizarin red S staining of osteoblasts from WT or *IRS-2*$^{-/-}$ calvariae cultured with and without insulin, IGF-I, or BMP-2 for 21 d. (D) Expression of Runx2, Lrp5, Id-1, type I collagen, ALP, osteocalcin, and osteopontin in cultured osteoblasts by semiquantitative RT-PCR.

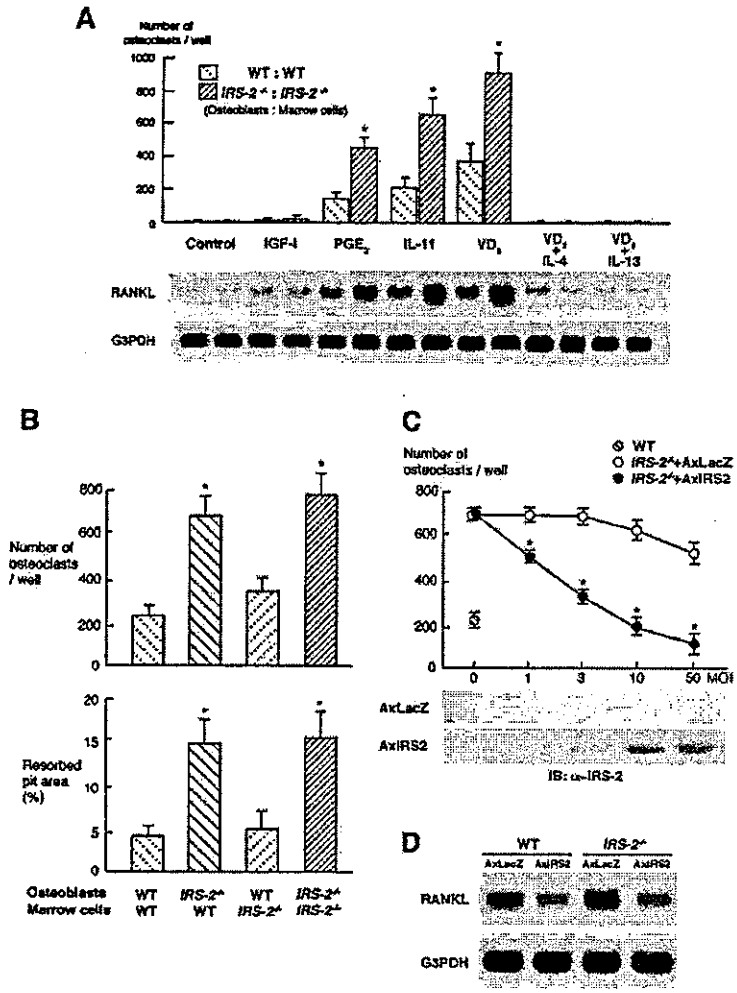


Figure 5. **Osteoclastogenesis was increased through the upregulation of RANKL expression in osteoblasts by IRS-2 deficiency.** (A) The number of TRAP-positive multinucleated osteoclasts formed in the coculture of osteoblasts and bone marrow cells from WT or *IRS-2*$^{-/-}$ littermates was counted after 6 d of culture with and without IGF-I, $PGE_2$, IL-11, $1,25(OH)_2D_3$ ($VD_3$), IL-4, or IL-13. Data are expressed as means (bars) ± SEMs (error bars) for eight wells/group. *, significantly different from WT cultures; $P < 0.01$ (top). Messenger RNA levels of RANKL in cultured WT and *IRS-2*$^{-/-}$ osteoblasts were determined by Northern blot analysis after 24 h of culture with and without the factors above (bottom). (B) The number of osteoclasts formed in the coculture of osteoblasts and bone marrow cells from WT and *IRS-2*$^{-/-}$ littermates in the presence of $1,25(OH)_2D_3$ (10 nM) (top) and the pit area resorbed by osteoclasts for an additional 48 h of the coculture on a dentine slice (bottom). Data are expressed as means (bars) ± SEMs (error bars) for 12 wells/group. *, significantly different from WT: WT culture; $P < 0.01$. (C) Restoration of osteoclastogenesis by reintroduction of IRS-2 in *IRS-2*$^{-/-}$ osteoblasts using an adenovirus vector carrying *IRS-2* gene (AxIRS2). *IRS-2*$^{-/-}$ osteoblasts infected with AxIRS2 or the control AxLacZ at indicated MOIs were cocultured with WT marrow cells in the presence of $1,25(OH)_2D_3$ for 6 d, and the number of TRAP-positive osteoclasts was counted (top). Data are expressed as means (symbols) ± SEMs (error bars) for eight wells/group. *, significantly different from AxLacZ-infected cultures; $P < 0.01$. IRS-2 protein level in *IRS-2*$^{-/-}$ cultured osteoblasts was determined by Western blotting after 2 d of infection of AxLacZ or AxIRS2 (bottom). (D) RANKL expression by introduction of IRS-2 in WT and *IRS-2*$^{-/-}$ osteoblasts. Osteoblasts infected with AxIRS2 or AxLacZ at 10 MOI were cultured in the presence of $1,25(OH)_2D_3$ for 24 h. RANKL mRNA level was determined by Northern blotting.

good correlation with that of osteoclastogenesis: RANKL induction by the resorptive factors was increased in *IRS-2*$^{-/-}$ osteoblasts compared with WT osteoblasts, whereas the inhibition by IL-4 and IL-13 was identical in both osteoblasts.

In the presence of $1,25(OH)_2D_3$, enhanced osteoclastogenesis in the coculture of *IRS-2*$^{-/-}$ osteoblasts and *IRS-2*$^{-/-}$ marrow cells (*IRS-2*$^{-/-}$:*IRS-2*$^{-/-}$) was normalized by replacing *IRS-2*$^{-/-}$ osteoblasts with WT osteoblasts (WT:*IRS-2*$^{-/-}$), but not by replacing *IRS-2*$^{-/-}$ marrow cells with WT marrow cells (*IRS-2*$^{-/-}$:WT) (Fig. 5 B, top). When the coculture was further performed on a dentine slice for 2 d, the area of resorption pits was correlated with the number of osteoclasts formed, indicating no difference of bone resorptive function between individual WT and *IRS-2*$^{-/-}$ osteoclasts (Fig. 5 B, bottom). These results indicate that the increase in bone resorption in *IRS-2*$^{-/-}$ mice is caused by the abnormality of osteoblasts to support osteoclastogenesis by inducing RANKL, but is not due to abnormalities of osteoclast progenitors or osteoclast function.

To further investigate the association between IRS-2 deficiency and the upregulation of osteoclastogenesis/RANKL expression, we examined their restoration by reintroduction of IRS-2 in *IRS-2*$^{-/-}$ osteoblasts using an adenovirus vector. When *IRS-2*$^{-/-}$ osteoblasts infected with an adenovirus vector carrying the *IRS-2* gene (AxIRS2) were cocultured with WT marrow cells in the presence of $1,25(OH)_2D_3$, osteoclastogenesis was decreased in a dose-dependent manner based on the AxIRS2 multiplicity of infection (MOI) and on the IRS-2 protein level determined by Western blotting, whereas the control adenovirus vector carrying the *LacZ* gene (AxLacZ) did not affect it (Fig. 5 C). Enhanced RANKL expression in cultured *IRS-2*$^{-/-}$ osteoblasts determined by Northern blotting was also decreased by AxIRS2 infection, but not by AxLacZ (Fig. 5 D). These results were reproducible in the stimulation of other bone resorptive factors, $PGE_2$ and IL-11 (unpublished data). It was therefore confirmed that the IRS-2 signaling pathway acts inhibitorily on enhanced osteoclastogenesis and RANKL expression in osteoblasts by these resorptive factors.

To confirm the role of IRS-2 intrinsic to osteoclastic cells, we investigated the differentiation and survival of osteoclasts using the M-BMMϕ culture system without supporting cells such as osteoblasts/stromal cells. Osteoclastogenesis from cultured M-BMMϕ in the presence of soluble RANKL for 3 d was similar between WT and *IRS-2*$^{-/-}$ cultures (674 ± 71 and 641 ± 83 cells/well, mean ± SEM of

12 wells, respectively). In addition, the survival of mature osteoclasts isolated from the M-BMMϕ culture did not differ between WT and *IRS-2*$^{-/-}$ osteoclasts (the average half life of 12 wells was 6.4 and 5.7 h, respectively). Hence, it was concluded that intrinsic IRS-2 signaling is not important for osteoclast function.

## Discussion

In vivo morphological analyses in this study demonstrated that *IRS-2*$^{-/-}$ mice exhibited osteopenia with decreased bone formation and increased bone resorption. In vitro cell culture analyses revealed that *IRS-2*$^{-/-}$ osteoblasts showed reduced ability of their differentiation and matrix synthesis. The increased osteoclastogenesis was due to the upregulation of RANKL in osteoblasts by IRS-2 deficiency. Although IRS-2, but not IRS-1, was expressed and phosphorylated by insulin/IGF-I in osteoclastic cells, intrinsic IRS-2 signaling in these cells was not important for their differentiation, function, or survival.

The present study revealed the difference in the physiological roles of IRS-1 and IRS-2 in bone metabolism. *IRS-2*$^{-/-}$ mice exhibited an uncoupling state with decreased bone formation and increased bone resorption, whereas our previous study found that *IRS-1*$^{-/-}$ mice displayed a decrease in both bone formation and bone resorption, indicating a low turnover osteopenia (Ogata et al., 2000). Hence, IRS-1 and IRS-2 seem to have opposite effects on osteoclastogenesis and RANKL expression in osteoblasts. The signaling specificity through the two IRSs may be accomplished by distinct phosphorylation patterns during interaction with various activated receptors (Sun et al., 1997). For example, phosphatidylinositol 3 (PI3) kinase activities in muscle and liver cells have functional differences in the ability of the two IRSs (Kadowaki et al., 1996; Burks and White, 2001). In this study, effects of bone resorptive factors, i.e., $PGE_2$, IL-11, or $1,25(OH)_2D_3$, on osteoclastogenesis and RANKL expression were shown to be partly inhibited by IRS-2 signaling, suggesting some convergence of signaling pathways between these factors and IRS-2. Because the main signaling pathways downstream of IRS-2 are known to be those of PI3 kinase and MAPK (Kadowaki et al., 1996; Withers et al., 1998; Burks and White, 2001), either pathway could conceivably be connected with the signaling of these resorptive factors. In fact, signalings of $PGE_2$ and IL-11 through their specific prostaglandin E and gp130 receptors, respectively, are known to utilize both PI3 kinase and MAPK (Fukada et al., 1999; Breyer et al., 2001). $1,25(OH)_2D_3$ signaling is also reported to be inhibited by MAPK pathway by the phosphorylation of retinoid X receptor α, the heterodimer of the nuclear vitamin D receptor, in human keratinocytes (Solomon et al., 1999). However, our preliminary study on the mechanism of RANKL induction failed to show the involvement of PI3 kinase, p42/44 MAPK, and p38 MAPK pathways because none of their inhibitors, LY294002, PD98059, or SB203580, altered the upregulation of the RANKL mRNA level by IRS-2 deficiency in cultured osteoblasts (unpublished data). We therefore speculate that signaling(s) other than PI3 kinase and these MAPKs may be involved in the suppression of RANKL expression and osteoclastogenesis by IRS-2. The next task ahead of us will be to elucidate the difference of signaling through IRS-1 and IRS-2 in osteoblasts.

IGF-I is a potent autocrine/paracrine factor for osteoblast proliferation and differentiation (Canalis, 1993). A relationship between bone density and IGF-I is suggested by a study showing a correlation of serum and skeletal IGF-I levels with bone density between two healthy inbred strains of mice (Rosen et al., 1997). In humans, accumulating evidence has suggested a positive correlation between the serum IGF-I level and bone density in postmenopausal women (Nicolas et al., 1994; Rosen, 1994; Reed et al., 1995; Canalis, 1997). The anabolic effect of insulin on bone formation may be primarily related to its ability to stimulate cell proliferation (Thomas et al., 1997). Streptozotocin-induced diabetic animals with impaired pancreatic insulin production lose bone rapidly, and this loss is offset by insulin replacement (Hough et al., 1981). Clinically, type 1 diabetes with insulin deficiency is associated with decreased bone mass; however, the change of bone mass in type 2 diabetic patients is controversial. Although previous reports demonstrated a decrease in bone mass in these latter patients, accumulating evidence has revealed that obese type 2 diabetic patients have normal or even increased bone mass (Kao et al., 1993; van Daele et al., 1995; Krakauer et al., 1997; Piepkorn et al., 1997). This might be due to the increased physical stress on the skeleton, or hyperinsulinemia seen in the earlier stage of type 2 diabetes. In fact, we previously demonstrated that patients with hyperinsulinemia are associated with the increased ossification of the spinal ligaments (Akune et al., 2001). Whether or not the response of bone cells to insulin is affected similarly to that of cells responsible for glucose metabolism, such as muscle, liver, and adipose tissue, in type 2 diabetic patients is an important point to be elucidated. Although the *IRS-2*$^{-/-}$ mice develop type 2 diabetes characterized by defects in both insulin action and insulin secretion, clinical studies on genetic polymorphisms have so far failed to show a pathogenic contribution of IRS-2 to the development of this condition (Sesti et al., 2001; Wang et al., 2001). Hence, we do not regard the *IRS-2*$^{-/-}$ mice as a model to define mechanisms of abnormalities of bone metabolism by type 2 diabetes. The mice may speak for themselves as a rare model showing an uncoupling state between bone formation and resorption.

In the histomorphometric analysis, osteoblast function was shown to be decreased by IRS-2 deficiency; however, the number of osteoblasts (Ob.S/BS) was either not affected or was increased (Table I). We speculate that this increase may be secondary to the upregulation of osteoclastic bone resorption through the coupling mechanism between osteoclasts and osteoblasts. In fact, in the osteoblast culture system in which osteoclastic cells were absent, cell proliferation was not different between WT and *IRS-2*$^{-/-}$ (Fig. 4 A), whereas cell differentiation and matrix synthesis were decreased in the *IRS-2*$^{-/-}$ culture. Hence, IRS-2 in osteoblasts seems to be related to the signaling of their differentiation and function, but not to their mitogenic or anti-apoptotic signaling directly.

The decrease in anabolic function of *IRS-2*$^{-/-}$ osteoblasts was seen not only in the culture with insulin or IGF-I but also in the control culture (Fig. 4, B, C, and D). This may possibly be due to the blockage of signals of endogenous

IGF-I acting as an autocrine/paracrine factor in the culture. The concentrations of IGF-I in the culture medium were 0.39 ± 0.12 and 0.48 ± 0.10 nM (mean ± SEM) in the control cultures of WT and *IRS-2*$^{-/-}$ osteoblasts, respectively. In addition, serum IGF-I levels were similar between WT and *IRS-2*$^{-/-}$ mice in the age from 8 to 16 wk, suggesting the absence of systemic compensation for impaired IGF-I bioactivity. Hence, the decreased bone formation in vivo in *IRS-2*$^{-/-}$ mice may be at least in part due to the deficit of anabolic signaling of endogenous IGF-I produced by osteoblasts acting as an autocrine/paracrine factor.

Intrinsic IRS-2 in osteoclastic cells was proven not to be important for their differentiation, function, or survival despite the fact that IRS-2 and receptors of IGF-I and insulin are expressed in these cells (Fiorelli et al., 1996; Hou et al., 1997; Thomas et al., 1998). Whether or not IGF-I or insulin directly acts on osteoclastic cells is controversial (Mochizuki et al., 1992; Hill et al., 1995), and we, in fact, failed to show the direct action of IGF-I or insulin in the culture of M-BMMϕ in the absence of osteoblasts/stromal cells (unpublished data). Furthermore, IRS-1 and IRS-2 are reported to regulate cell apoptosis through phosphorylation of Bcl-2 in a myeloma cell line (Ueno et al., 2000), however, these proteins did not affect osteoclast survival in our previous and present studies (Ogata et al., 2000). Hence, IGF-I/insulin and IRS signalings are likely to regulate bone resorption more predominantly by their indirect actions through osteoblasts/stromal cells than by their direct actions on osteoclastic cells.

Clinically, loss of anabolic actions of insulin and IGF-I on bone metabolism is implied to cause various bone metabolic diseases. Taken together with our previous study, we hereby propose that these anabolic actions are maintained as an integration of two proteins that have distinct biological roles in osteoblasts, IRS-1 and IRS-2. The former is essential to maintain bone turnover by upregulating anabolic function and RANKL expression, whereas the latter is needed to retain the predominance of the anabolic function over the catabolic function. Distinct regulation of these two IRS proteins in osteoblasts may play a key role in controlling bone metabolism and maintaining bone homeostasis.

## Materials and methods

### Animals

In each experiment, homozygous WT and *IRS-2*$^{-/-}$ mice that were littermates generated from the intercross between heterozygous mice were compared. All experiments were performed on male mice unless otherwise described. All experiments were performed according to the protocol approved by the Animal Care and Use Committee of the University of Tokyo.

### Analysis of skeletal morphology

Bone radiograph was taken with a soft X-ray apparatus (SOFTEX; CMB-2). Three-dimensional CT scan was taken using a composite X-ray analyzing system (NX-HCP; NS-ELEX Inc.). BMD was measured by single energy X-ray absorptiometry using a bone mineral analyzer (DCS-600R; Aloka Co.). All histological analyses were performed using 8-wk-old WT and *IRS-2*$^{-/-}$ littermates. For Villanueva-Goldner staining, tibiae were fixed with ethanol, embedded in methyl methacrylate, and sectioned in 6-μm slices. For double labeling, mice were injected subcutaneously with 8 mg/kg body weight of calcein at 10 and 3 d before sacrifice. TRAP-positive cells were stained at pH 5.0 in the presence of L(+)-tartaric acid using naphthol AS-MX phosphate (Sigma-Aldrich) in *N,N*-dimethyl formamide as the substrate. The specimens were subjected to histomorphometric analyses using an image analyzer (System Supply Co.). Parameters for the trabecular bone were measured in an area 1.2 mm in length from 0.5 mm below the growth plate at the proximal metaphysis of the tibiae. Parameters for the cortex bone were measured at the midshaft of the tibiae. The thickness of the growth plate was measured at the proximal tibiae.

### Immunohistochemistry

After perfusion of 4-wk-old WT mice with 4% buffered paraformaldehyde, tibiae were removed and immersed in the same fixative for paraffin sections. 3-mm-thick paraffin sections were treated with 0.3% hydrogen peroxide in PBS. After blocking with 1% albumin in PBS, they were incubated with a rabbit polyclonal anti–mouse IRS-2 antibody (Upstate Biotechnology) at a dilution of 1:50 for 24 h at 4°C. The sections were incubated with HRP-conjugated goat antibodies against rabbit IgG (Dakopatts) for 1 h at room temperature. After washing with PBS, they were immersed in a diaminobenzidine solution for 10 min at room temperature to observe any immunoreactivity. As a control, we used a rabbit nonimmune serum (Upstate Biotechnology) of the same dilution instead of the primary antibody.

### In vitro osteoblast cultures

Osteoblasts were isolated from calvariae of neonatal WT and *IRS-2*$^{-/-}$ littermates. Calvariae were digested for 10 min at 37°C in an enzyme solution containing 0.1% collagenase and 0.2% dispase five times. Cells isolated by the last four digestions were combined as an osteoblast population and cultured in αMEM containing 10% FBS. For cell proliferation assay, primary osteoblasts were inoculated at a density of 1 × 10$^4$ cells/well in a 24-multiwell plate, cultured in the same medium for 48 h, and deprived of serum for 12 h before adding the experimental medium with and without IGF-I (10 nM), insulin (100 nM), or FGF-2 (1 nM). Incorporation of [$^3$H]thymidine (1 μCi/ml in the medium) added for the final 3 h was measured after 24 h of culture. For ALP activity measurement, primary osteoblasts were inoculated at a density of 1 × 10$^4$ cells/well in a 24-multiwell plate and cultured in αMEM containing 10% FBS and 50 μg/ml ascorbic acid with and without IGF-I (10 nM), insulin (100 nM), or BMP-2 (30 ng/ml). At 14 d of culture, cells were sonicated in 10 mM Tris-HCl buffer (pH 8.0) containing 1 mM $MgCl_2$ and 0.5% Triton X-100. ALP activity in the lysate was measured using a Wako ALP kit (Wako Pure Chemical Industry, Ltd.). The protein content was determined using BCA protein assay reagent (Pierce Chemical Co.). For Alizarin red S staining, osteoblasts were inoculated at a density of 5 × 10$^4$ cells/well in a six-multiwell plate in αMEM containing 10% FBS and 50 μg/ml ascorbic acid and 10 mM β-glycerophosphate. At day 21 after confluency, cultured cells were fixed in 10% buffered formalin and stained for 10 min with 2% Alizarin red S (pH 4.0) (Sigma-Aldrich).

### Coculture of osteoblasts and bone marrow cells

Bone marrow cells were collected from long bones of 8-wk-old WT or *IRS-2*$^{-/-}$ littermates. TRAP-positive multinucleated osteoclasts were generated by coculturing osteoblasts (1 × 10$^4$ cells/well) and bone marrow cells (5 × 10$^5$ cells/well) derived from either WT or *IRS-2*$^{-/-}$ littermates in a 24-multiwell plate in αMEM containing 10% FBS for 6 d with and without IGF-I (10 nM), 1,25(OH)$_2$D$_3$ (10 nM), $PGE_2$ (100 nM), IL-11 (10 ng/ml), IL-4 (100 ng/ml), or IL-13 (100 ng/ml). Cells positively stained for TRAP containing more than three nuclei were counted as osteoclasts. To determine bone resorption activity, osteoclasts formed by the coculture on 0.24% collagen gel coated on 100-mm dishes were digested with 0.2% collagenase solution, and a 1/50 aliquot including osteoclasts was seeded on a dentine slice. After 48 h of culture in αMEM containing 10% FBS, the total area of pits stained with 0.5% toluidine blue was evaluated using an image analyzer.

### M-BMMϕ culture

We used the M-BMMϕ culture system as described previously (Kobayashi et al., 2000). In brief, bone marrow cells from WT or *IRS-2*$^{-/-}$ mice were seeded at a density of 3 × 10$^5$ cells/well in a 24-multiwell plate and cultured in αMEM containing 10% FBS with M-CSF (100 ng/ml). After culturing for 3 d, adherent cells (M-BMMϕ) were further cultured with M-CSF (100 ng/ml) and soluble RANKL (100 ng/ml) for 3 d. TRAP-positive osteoclasts were counted. To determine the survival, osteoclasts generated as above were deprived of M-CSF/soluble RANKL and cultured for an additional 48 h. At 3, 6, 12, 24, and 48 h, the number of TRAP-positive and trypan blue–negative osteoclasts was counted.

### Generation of adenoviruses and gene transfer

The recombinant adenovirus vector carrying *IRS-2* gene containing CAG (cytomegalovirus immediate early enhancer + chicken actin promoter + rabbit globin poly A signal) promoter was constructed using the Adenovi-

rus Expression Vector Kit (Takara Shuzo Co., Ltd.) following the manufacturer's protocol. The adenovirus vector carrying the *β-galactosidase* gene (AxLacZ) was provided by Dr. I. Saito (University of Tokyo). *IRS-2*$^{-/-}$ osteoblasts were seeded at a density of $1 \times 10^4$ cells/well in a 24-multiwell plate and treated with viral suspensions for 1 h at 37°C at a concentration indicated as the MOI for 2 d. Infection efficiency was confirmed by β-galactosidase assay using X-gal as a substrate, and Western blot analysis of IRS-2. IRS-2 protein level was also confirmed by Western blotting. For the experiment of osteoclastogenesis, they were then washed three times with PBS, and WT bone marrow cells were added at a density of $5 \times 10^5$ cells/well with and without $1,25(OH)_2D_3$ (10 nM), $PGE_2$ (100 nM), or IL-11 (10 ng/ml) and cocultured for 6 d. The number of TRAP-positive osteoclasts was counted. For the experiment of RANKL expression, osteoblasts infected with 10 MOI of AxIRS2 or AxLacZ were further cultured with and without the resorptive factors above for 24 h, and the mRNA level was determined by Northern blotting.

### Immunoprecipitation and Western blot analysis

After stimulation by IGF-I (10 nM) or insulin (100 nM), cultured cells were lysed with TNE buffer (10 mM Tris-HCl, 150 mM NaCl, 1% NP-40, 1 mM EDTA, 10 mM NaF, 2 mM $Na_3VO_4$, 1 mM aminoethyl-benzenesulfonyl fluoride, and 10 μg/ml aprotinin). Immunoprecipitation was performed using antibodies either noncovalently bound or conjugated to protein G–Sepharose (GIBCO BRL). Equivalent amounts (20 μg) of cell lysate were immunoprecipitated with a polyclonal anti–mouse IRS-2 antibody (Upstate Biotechnology) for 4 h at 4°C. Each cell lysate or immunoprecipitated protein containing an equivalent amount of protein was electrophoresed by 8% SDS-PAGE and transferred to nitrocellulose membrane. After blocking with 5% albumin solution, they were incubated with an antiphosphotyrosine antibody (Upstate Biotechnology). Immunoreactive bands were stained using the ECL chemiluminescence reaction (Amersham Biosciences).

### Northern blotting and semiquantitative RT-PCR

For Northern blot analysis, osteoblasts were cultured in αMEM containing 10% FBS with and without IGF-I (10 nM), $1,25(OH)_2D_3$ (10 nM), $PGE_2$ (100 nM), IL-11 (10 ng/ml), IL-4 (100 ng/ml), or IL-13 (100 ng/ml). Total RNA was extracted using an ISOGEN kit (Wako Pure Chemical). 30 μg of total RNA was electrophoresed in 1.2% agarose–formaldehyde gels and transferred onto nylon membrane filters (Hybond-N; Amersham Biosciences). The membranes were hybridized for 12 h at 42°C with cDNA probes for mouse RANKL, which were labeled using a multirandom primer oligonucleotide labeling kit (Boehringer) and [$^{32}$P]dCTP. Semiquantitative RT-PCR was performed within an exponential phase of the amplification. Total mRNA (1 μg) was reverse transcribed using Super Script reverse transcriptase (Takara Shuzo Co., Ltd.) with random hexamer (Takara Shuzo Co., Ltd.), and 5% of the reaction mixture was amplified with LA-Taq DNA polymerase (Takara Shuzo Co., Ltd.) using the following primer pairs: 5'-GCAGCCCCACCTGCCTCGAAAGGTAGACAC-3' and 5'-CAGCAATGCCTGTCCGCATGTCAGCATAGC-3' for IRS-1; 5'-GAAGACAGTGGGTACATGCGAATG-3' and 5'-CCTCATGGAGGAAGGCACTGCTG-3' for IRS-2; 5'-CATGTAGGCCATGAGGTCCACCAC-3' and 5'-TGAAGGTCGGTGTGAACGGATTTGGC-3' for G3PDH; 5'-GCACCGCCGAGATGGACTGCTGAA-3' and 5'-GGCGGAAAGAGGATGGAGGTGACG-3' for Runx2; 5'-CCTGCTGCCTCCCTGTAA-3' and 5'-CTTCACCGCTCACATTTCTC-3' for Lrp5; 5'-ACTGAGGGACCAGATGGACTCCAG-3' and 5'-GCCAGTGATCATTGTAATATACA-3' for Id-1; 5'-CTGGGATGGACAAGGAGAGT-3' and 5'-AAGGCTGAGAGGCTATGGTG-3' for type I collagen; 5'-GCCCTCTCCAAGACATATA-3' and 5'-CCATGATCACGTCGATATCC-3' for ALP; 5'-AGTCGACATGAGATTGGCAGTGATTTGC-3' and 5'-ACTCGAGGCCTCTTCTTTAGTTGACCTC-3' for osteopontin; 5'-TCGTTTCTTTCTGCTGGTCA-3' and 5'-CTTATTGCCCTCCTGCTTGG-3' for osteocalcin; 5'-GCATCGCTCTGTTCCTGTA-3' and 5'-GTGCTCCCTCCTTTCATCA-3' for RANKL; 5'-TCCTGGCACCTACCTAAAACAGCA-3' and 5'-CTACACTCTCGGCATTCACTTTGG-3' for osteoprotegerin; and 5'-CATTCAGCTATCCTGGCCACCTTC-3' and 5'-CATCCACATGGTTGGGAAGTTCTG-3' for MMP-13. Up to 25 cycles of amplification were performed with a PerkinElmer PCR thermal cycler (PE-2400) at 94°C for 30 s, at 52–60°C for 60 s, and at 72°C for 90 s.

### Statistical analysis

Means of groups were compared by ANOVA and significance of differences was determined by post-hoc testing using Bonferroni's method.

We thank the hard tissue research team at Kureha Chemical Co., Ltd. for technical assistance, and Dr. Ung-Il Chung (University of Tokyo) for helpful discussion.

This work was supported by grants-in-aid for scientific research from the Japanese Ministry of Education, Science, Sports, and Culture (Nos. 11470301 and 12137201), the Uehara Memorial Foundation, and the Takeda Science Foundation.

Submitted: 9 April 2002
Revised: 8 August 2002
Accepted: 30 August 2002

## References

Akune, T., N. Ogata, A. Seichi, I. Ohnishi, K. Nakamura, and H. Kawaguchi. 2001. Insulin secretory response is positively associated with the extent of ossification of the posterior longitudinal ligament of the spine. *J. Bone Joint Surg. Am.* 83:1537–1544.

Araki, E., M.A. Lipes, M.E. Patti, J.C. Bruning, B. Haag, III, R.S. Johnson, and C.R. Kahn. 1994. Alternative pathway of insulin signaling in mice with targeted disruption of the *IRS-1* gene. *Nature.* 372:186–190.

Breyer, R.M., C.K. Bagdassarian, S.A. Myers, and M.D. Breyer. 2001. Prostanoid receptors: subtypes and signaling. *Annu. Rev. Pharmacol. Toxicol.* 41:661–690.

Bruning, J.C., J. Winnay, B. Cheatham, and C.R. Kahn. 1997. Differential signaling by insulin receptor substrate 1 (IRS-1) and IRS-2 in IRS-1-deficient cells. *Mol. Cell. Biol.* 17:1513–1521.

Burks, D.J., and M.F. White. 2001. IRS proteins and β-cell function. *Diabetes.* 50: S140–S145.

Burks, D.J., J.F. de Mora, M. Schubert, D.J. Withers, M.G. Myers, H.H. Towery, S.L. Altamuro, C.L. Flint, and M.F. White. 2000. IRS-2 pathways integrate female reproduction and energy homeostasis. *Nature.* 407:377–382.

Canalis, E. 1993. Insulin-like growth factors and the local regulation of bone formation. *Bone.* 14:273–276.

Canalis, E. 1997. Insulin-like growth factors and osteoporosis. *Bone.* 21:215–216.

Fiorelli, G., L. Formigli, O.S. Zecchi, F. Gori, A. Falchetti, A. Morelli, A. Tanini, S. Benvenuti, and M.L. Brandi. 1996. Characterization and function of the receptor for IGF-I in human preosteoclastic cells. *Bone.* 18:269–276.

Fukada, T., Y. Yoshida, K. Nishida, T. Ohtani, T. Shirogane, M. Hibi, and T. Hirano. 1999. Signaling through Gp130: toward a general scenario of cytokine action. *Growth Factors.* 17:81–91.

Hill, P.A., J.J. Reynolds, and M.C. Meikle. 1995. Osteoblasts mediate insulin-like growth factor-I and -II stimulation of osteoclast formation and function. *Endocrinology.* 136:124–131.

Hou, P., T. Sato, W. Hofstetter, and N.T. Foged. 1997. Identification and characterization of the insulin-like growth factor I receptor in mature rabbit osteoclasts. *J. Bone Miner. Res.* 12:534–540.

Hough, S., L.V. Avioli, M.A. Bergfeld, M.D. Fallon, E. Slatopolsky, and S.L. Teitelbaum. 1981. Correction of abnormal bone and mineral metabolism in chronic streptozotocin-induced diabetes mellitus in the rat by insulin therapy. *Endocrinology.* 108:2228–2234.

Kadowaki, T., K. Tobe, R. Honda-Yamamoto, H. Tamemoto, Y. Kaburagi, K. Momomura, K. Ueki, Y. Takahashi, T. Yamauchi, Y. Akanuma, and Y. Yazaki. 1996. Signal transduction mechanism of insulin and insulin-like growth factor-1. *Endocr. J.* 43:S33–S41.

Kao, C.H., C.T. Tsou, C.C. Chen, and S.J. Wang. 1993. Bone mineral density in patients with noninsulin-dependent diabetes mellitus by dual photon absorptiometry. *Nucl. Med. Commun.* 14:373–377.

Karsenty, G. 2001. Minireview: transcriptional control of osteoblast differentiation. *Endocrinology.* 142:2731–2733.

Kobayashi, K., N. Takahashi, E. Jimi, N. Udagawa, M. Takami, S. Kotake, N. Nakagawa, M. Kinosaki, K. Yamaguchi, N. Shima, et al. 2000. Tumor necrosis factor α stimulates osteoclast differentiation by a mechanism independent of the ODF/RANKL-RANK interaction. *J. Exp. Med.* 191:275–286.

Krakauer, J.C., M.J. McKenna, D.S. Rao, and F.W. Whitehouse. 1997. Bone mineral density in diabetes. *Diabetes Care.* 20:1339–1340.

Kubota, N., K. Tobe, Y. Terauchi, K. Eto, T. Yamauchi, R. Suzuki, Y. Tsubamoto, K. Komeda, R. Nakano, H. Miki, et al. 2000. Disruption of insulin receptor substrate 2 causes type 2 diabetes because of liver insulin resistance and lack of compensatory β-cell hyperplasia. *Diabetes.* 49:1880–1889.

Laron, Z., B. Klinger, and A. Silbergeld. 1999. Patients with Laron syndrome have osteopenia/osteoporosis. *J. Bone Miner. Res.* 14:156–157.

Lavan, B.E., V.R. Fantin, E.T. Chang, W.S. Lane, S.R. Keller, and G.E. Lienhard. 1997a. A novel 160-kDa phosphotyrosine protein in insulin-treated embryonic kidney cells is a new member of the insulin receptor substrate family. *J. Biol. Chem.* 272:21403–21407.

Lavan, B.E., W.S. Lane, and G.E. Lienhard. 1997b. The 60-kDa phosphotyrosine protein in insulin-treated adipocytes is a new member of the insulin receptor substrate family. *J. Biol. Chem.* 272:11439–11443.

Mochizuki, H., Y. Hakeda, N. Wakatsuki, N. Usui, S. Akashi, T. Sato, K. Tanaka, and M. Kumegawa. 1992. Insulin-like growth factor-I supports formation and activation of osteoclasts. *Endocrinology.* 131:1075–1080.

Nicolas, V., A. Prewett, P. Bettica, S. Mohan, R.D. Finkelman, D.J. Baylink, and J.R. Farley. 1994. Age-related decreases in insulin-like growth factor-I and transforming growth factor-β in femoral cortical bone from both men and women: implications for bone loss with aging. *J. Clin. Endocrinol. Metab.* 78:1011–1016.

Ogata, N., D. Chikazu, N. Kubota, Y. Terauchi, K. Tobe, Y. Azuma, T. Ohta, T. Kadowaki, K. Nakamura, and H. Kawaguchi. 2000. Insulin receptor substrate-1 in osteoblast is indispensable for maintaining bone turnover. *J. Clin. Invest.* 105:935–943.

Ogata, T., J.M. Wozney, R. Benezra, and M. Noda. 1993. Bone morphogenetic protein 2 transiently enhances expression of a gene, Id (inhibitor of differentiation), encoding a helix-loop-helix molecule in osteoblast-like cells. *Proc. Natl. Acad. Sci. USA.* 90:9219–9222.

Patel, M.S., and G. Karsenty. 2002. Regulation of bone formation and vision by LRP5. *N. Engl. J. Med.* 346:1572–1574.

Piepkorn, B., P. Kann, T. Forst, J. Andreas, A. Pfutzner, and J. Beyer. 1997. Bone mineral density and bone metabolism in diabetes mellitus. *Horm. Metab. Res.* 29:584–591.

Reed, B.Y., J.E. Zerwekh, K. Sakhaee, N.A. Breslau, F. Gottschalk, and C.Y. Pak. 1995. Serum IGF-I is low and correlated with osteoblastic surface in idiopathic osteoporosis. *J. Bone Miner. Res.* 10:1218–1224.

Rosen, C.J. 1994. Growth hormone, insulin-like growth factors, and the senescent skeleton: Ponce de Leon's fountain revisited? *J. Cell. Biochem.* 56:348–356.

Rosen, C.J., H.P. Dimai, D. Vereault, L.R. Donahue, W.G. Beamer, J. Farley, S. Linkhart, T. Linkhart, S. Mohan, and D.J. Baylink. 1997. Circulating and skeletal insulin-like growth factor-I (IGF-I) concentrations in two inbred strains of mice with different bone mineral densities. *Bone.* 21:217–223.

Scopes, J., H.M. Massey, H. Ebrahim, M.A. Horton, and A.M. Flanagan. 2001. Interleukin-4 and interleukin-13: bidirectional effects on human osteoclast formation. *Bone.* 29:203–208.

Sesti, G., M. Federici, M.L. Hribal, D. Lauro, P. Sbraccia, and R. Lauro. 2001. Defects of the insulin receptor substrate (IRS) system in human metabolic disorders. *FASEB J.* 15:2099–2111.

Solomon, C., J.H. White, and R. Kremer. 1999. Mitogen-activated protein kinase inhibits 1,25-dihydroxyvitamin D3-dependent signal transduction by phosphorylating human retinoid X receptor α. *J. Clin. Invest.* 103:1729–1735.

Suda, T., N. Takahashi, N. Udagawa, E. Jimi, M.T. Gillespie, and T.J. Martin. 1999. Modulation of osteoclast differentiation and function by the new members of the tumor necrosis factor receptor and ligand families. *Endocr. Rev.* 20:345–357.

Sun, X.J., S. Pons, L.M. Wang, Y. Zhang, L. Yenush, D. Burks, M.G. Myers, Jr., E. Glasheen, N.G. Copeland, N.A. Jenkins, et al. 1997. The IRS-2 gene on murine chromosome 8 encodes a unique signaling adapter for insulin and cytokine action. *Mol. Endocrinol.* 11:251–262.

Tamemoto, H., T. Kadowaki, K. Tobe, T. Yagi, H. Sakura, T. Hayakawa, Y. Terauchi, K. Ueki, Y. Kaburagi, S. Satoh, et al. 1994. Insulin resistance and growth retardation in mice lacking insulin receptor substrate-1. *Nature.* 372: 182–186.

Thomas, D.M., D.K. Hards, S.D. Rogers, K.W. Ng, and J.D. Best. 1997. Insulin and bone, clinical and scientific view. *Endocrinol. Metab.* 4:5–17.

Thomas, D.M., N. Udagawa, D.K. Hards, J.M. Quinn, J.M. Moseley, D.M. Findlay, and J.D. Best. 1998. Insulin receptor expression in primary and cultured osteoclast-like cells. *Bone.* 23:181–186.

Tobe, K., R. Suzuki, M. Aoyama, T. Yamauchi, J. Kamon, N. Kubota, Y. Terauchi, J. Matsui, Y. Akanuma, S. Kimura, et al. 2001. Increased expression of the sterol regulatory element-binding protein-1 gene in insulin receptor substrate-2($^{-/-}$) mouse liver. *J. Biol. Chem.* 276:38337–38340.

Uchida, M., M. Shima, T. Shimoaka, A. Fujieda, K. Obara, H. Suzuki, Y. Nagai, T. Ikeda, H. Yamato, and H. Kawaguchi. 2000. Regulation of matrix metalloproteinases (MMPs) and tissue inhibitors of metalloproteinases (TIMPs) by bone resorptive factors in osteoblastic cells. *J. Cell. Physiol.* 185:207–214.

Ueno, H., E. Kondo, R. Yamamoto-Honda, K. Tobe, T. Nakamoto, K. Sasaki, K. Mitani, A. Furusaka, T. Tanaka, Y. Tsujimoto, et al. 2000. Association of insulin receptor substrate proteins with Bcl-2 and their effects on its phosphorylation and antiapoptotic function. *Mol. Biol. Cell.* 11:735–746.

van Daele, P.L., R.P. Stolk, H. Burger, D. Algra, D.E. Grobbee, A. Hofman, J.C. Birkenhager, and H.A. Pols. 1995. Bone density in non-insulin-dependent diabetes mellitus. The Rotterdam Study. *Ann. Intern. Med.* 122:409–414.

Wang, H., J. Rissanen, R. Miettinen, P. Karkkainen, P. Kekalainen, J. Kuusisto, L. Mykkanen, P. Karhapaa, and M. Laakso. 2001. New amino acid substitutions in the *IRS-2* gene in Finnish and Chinese subjects with late-onset type 2 diabetes. *Diabetes.* 50:1949–1951.

Wang, H.Y., J. Zamorano, and A.D. Keegan. 1998. A role for the insulin-interleukin (IL)-4 receptor motif of the IL-4 receptor α-chain in regulating activation of the insulin receptor substrate 2 and signal transducer and activator of transcription 6 pathways. Analysis by mutagenesis. *J. Biol. Chem.* 273:9898–9905.

White, M.F. 1998. The IRS-signaling system: a network of docking proteins that mediate insulin action. *Mol. Cell. Biochem.* 182:3–11.

Withers, D.J., J.S. Gutierrez, H. Towery, D.J. Burks, J.M. Ren, S. Previs, Y. Zhang, D. Bernal, S. Pons, G.I. Shulman, et al. 1998. Disruption of IRS-2 causes type 2 diabetes in mice. *Nature.* 391:900–904.

Wurster, A.L., D.J. Withers, T. Uchida, M.F. White, and M.J. Grusby. 2002. Stat6 and IRS-2 cooperate in interleukin 4 (IL-4)-induced proliferation and differentiation but are dispensable for IL-4-dependent rescue from apoptosis. *Mol. Cell. Biol.* 22:117–126.

Yamauchi, T., K. Tobe, H. Tamemoto, K. Ueki, Y. Kaburagi, R. Yamamoto-Honda, Y. Takahashi, F. Yoshizawa, S. Aizawa, Y. Akanuma, et al. 1996. Insulin signaling and insulin actions in the muscles and livers of insulin-resistant, insulin receptor substrate 1-deficient mice. *Mol. Cell. Biol.* 16:3074–3084.

Yano, K., E. Tsuda, N. Washida, F. Kobayashi, M. Goto, A. Harada, K. Ikeda, K. Higashio, and Y. Yamada. 1999. Immunological characterization of circulating osteoprotegerin/osteoclastogenesis inhibitory factor: increased serum concentrations in postmenopausal women with osteoporosis. *J. Bone Miner. Res.* 14:518–527.

THE JOURNAL OF BIOLOGICAL CHEMISTRY
Vol. 277, No. 9, Issue of March 1, pp. 7493–7500, 2002
Printed in U.S.A.


# Regulation of Osteoblast, Chondrocyte, and Osteoclast Functions by Fibroblast Growth Factor (FGF)-18 in Comparison with FGF-2 and FGF-10*

Received for publication, September 7, 2001, and in revised form, December 7, 2001
Published, JBC Papers in Press, December 11, 2001, DOI 10.1074/jbc.M108653200

**Takashi Shimoaka‡, Toru Ogasawara‡, Akiko Yonamine§, Daichi Chikazu‡, Hirotaka Kawano‡, Kozo Nakamura‡, Nobuyuki Itoh§, and Hiroshi Kawaguchi‡¶**

*From the ‡Department of Orthopedic Surgery, Faculty of Medicine, University of Tokyo, Hongo 7-3-1, Bunkyo, Tokyo 113-8655, Japan and §Department of Genetic Biochemistry, Kyoto University Graduate School of Pharmaceutical Sciences, Yoshida-Shimoadachi 46-29, Sakyo, Kyoto 606-8501, Japan*

**This study investigated the actions of fibroblast growth factor (FGF)-18, a novel member of the FGF family, on osteoblasts, chondrocytes, and osteoclasts and compared them with those of FGF-2 and FGF-10. FGF-18 stimulated the proliferation of cultured mouse primary osteoblasts, osteoblastic MC3T3-E1 cells, primary chondrocytes, and prechondrocytic ATDC5 cells, although it inhibited the differentiation and matrix synthesis of these cells. FGF-18 up-regulated the phosphorylation of extracellular signal-regulated kinase in both osteoblasts and chondrocytes and up-regulated the phosphorylation of p38 mitogen-activated protein kinase only in chondrocytes. FGF-18 mitogenic actions were blocked by a specific inhibitor of extracellular signal-regulated kinase in both osteoblasts and chondrocytes and by a specific inhibitor of p38 mitogen-activated protein kinase in chondrocytes. With regard to the action of FGF-18 on bone resorption, FGF-18 not only induced osteoclast formation through receptor activator of nuclear factor-κB ligand and cyclooxygenase-2 but also stimulated osteoclast function to form resorbed pits on a dentine slice in the mouse coculture system. All these effects of FGF-18 bore a close resemblance to those of FGF-2, whereas FGF-10 affects none of these cells. FGF-18 may therefore compensate for the action of FGF-2 on bone and cartilage.**

Fibroblast growth factors (FGFs)[1] are potent mitogens for a wide variety of cells of mesenchymal and neuroectodermal origin (1). FGFs also play a role in the differentiation of a variety of cells and are involved in morphogenesis, angiogenesis, and development. The FGF family now consists of 23 members, FGF-1 to FGF-23, and there are 4 structurally related high-affinity receptors (FGFR1 to FGFR4) belonging to receptor tyrosine kinases that have an intrinsic protein tyrosine kinase activity and elicit tyrosine autophosphorylation of the receptor (1, 2). Recent reports showing that mutations of FGFRs cause several genetic diseases with severe impairment of bone and cartilage formation, such as achondroplasia (3, 4) and thanatophoric dysplasia type II (5), indicate the essential role of FGF signalings on bone and cartilage metabolism.

Among FGFs, FGF-2 is well known as a potent regulator of functions of bone and cartilage cells. It is produced by cells of osteoblastic lineage, accumulated in bone matrix, and acts as an autocrine/paracrine factor for bone cells (6–8). We and others have reported that the exogenous application of FGF-2 has stimulatory effects on bone formation in several *in vivo* models as a pharmacological action (9–11). In addition, the *Fgf-2*-deficient mouse exhibits decreased bone mass and bone formation, although these changes were rather moderate (12). Paradoxically, FGF-2 is also known as a potent stimulator of bone resorption (13–17) and is involved in joint destruction of rheumatoid arthritis patients (18). The stimulatory effect of FGF-2 on osteoclast formation is mediated by the induction of cyclooxygenase-2, a main regulatory enzyme for prostaglandin production in bone, and receptor activator of nuclear factor-κB ligand (RANKL), a key membrane-associated molecule regulating osteoclast differentiation, in osteoblasts (13–15, 17). Other than this indirect action through the mediation of osteoblasts, we recently reported that FGF-2 acts directly on mature osteoclasts to stimulate bone resorption (15, 16).

Another FGF, FGF-10, was recently cloned and shown to be expressed predominantly in the embryo and adult lung (19). Further investigation revealed that it emanated from the prospective limb mesoderm to serve as an endogenous initiator for limb bud formation and that ectopic application of FGF-10 induced FGF-8 expression in the adjacent ectoderm (20). FGF-10 was recently shown to be essential for limb bud formation because the *Fgf-10*-deficient mouse exhibited complete truncation of limbs (21). However, the effect of FGF-10 on bone and cartilage cells remains unknown.

Two different groups have recently cloned a novel member of the FGF family, designated FGF-18 (22, 23). Sequence comparison indicates that FGF-18 is highly conserved between humans and mice and is most homologous to FGF-8 and FGF-17 among the FGF family members. FGF-18 is expressed primarily in the adult lungs and kidneys as well as in several discrete regions at embryonic days 14.5 and 19.5. The temporal and spatial patterns of FGF-18 expression in embryos are quite different from those of FGF-8 and FGF-17, suggesting that FGF-18 is a unique secreted signaling molecule in several adult

* This work was supported by Grant-in-aid for Scientific Research 12470303 from the Japanese Ministry of Education, Science, Sports, Culture and Technology (to H. Kawaguchi) and a grant from the Human Frontier Science Program, France (to N. I.). None of the authors have financial interests in Amgen. The costs of publication of this article were defrayed in part by the payment of page charges. This article must therefore be hereby marked "*advertisement*" in accordance with 18 U.S.C. Section 1734 solely to indicate this fact.

¶ To whom correspondence should be addressed. Tel.: 81-3-3815-5411, Ext. 30473 or 33376; Fax: 81-3-3818-4082; E-mail: kawaguchi-ort@h.u-tokyo.ac.jp.

[1] The abbreviations used are: FGF, fibroblast growth factor; FGFR, fibroblast growth factor receptor; RANKL, receptor activator of nuclear factor-κB ligand; BMP, bone morphogenetic protein; αMEM, α modified minimum essential medium; FBS, fetal bovine serum; ERK, extracellular signal-regulated kinase; MAPK, mitogen-activated protein kinase; JNK, c-Jun N-terminal kinase; PBS, phosphate-buffered saline.

and developing tissues. It is a pleiotropic growth factor that stimulates proliferation in some tissues such as the liver and small intestine (23, 24); however, its role in bone and cartilage remains undetermined. This study therefore investigated the actions of FGF-18 on cultured osteoblasts, chondrocytes, and osteoclasts and compared them with those of FGF-2 and FGF-10.

## EXPERIMENTAL PROCEDURES

*Materials*—Neonatal and 8-week-old ddY mice were purchased from Shizuoka Laboratories Animal Center (Shizuoka, Japan). Rat recombinant FGF-18 was generously provided by Amgen Inc. (Thousand Oaks, CA), human recombinant FGF-2 was provided by Kaken Pharmaceutical Co., Ltd. (Chiba, Japan), rat recombinant FGF-10 was provided by Sumitomo Pharmaceutical Co., Ltd. (Osaka, Japan), bone morphogenetic protein (BMP)-2 was provided by Yamanouchi Pharmaceutical Co., Ltd. (Tokyo, Japan), NS-398 was provided by Taisho Pharmaceutical Co., Ltd. (Tokyo), and osteoprotegerin was provided by Snow Brand Milk Products Co., Ltd. (Tochigi, Japan). α Modified minimum essential medium (αMEM) was purchased from Invitrogen, and fetal bovine serum (FBS) was from the Cell Culture Laboratory (Cleveland, OH). Bacterial collagenase and 1,25$(OH)_2$ vitamin $D_3$ were purchased from Wako Pure Chemicals Co. (Osaka, Japan), and dispase was purchased from Nitta Gelatin Co. (Osaka, Japan). Polyclonal rabbit antibody against phosphotyrosine was obtained from Upstate Biotechnology Inc. (Lake Placid, NY). Polyclonal rabbit antibodies against phospho-ERK, phospho-p38 MAPK, phospho-JNK, and PD98059 (2′-amino-3′-methoxyflanone) were obtained from New England Biolabs, Inc. (Beverly, MA). SB203580 (4-(4-fluorophenyl)-2-(4-methylsulfinylphenyl)-5-(4-pyridyl)1*H*-imidazole) and Pronase were purchased from Calbiochem-Novabiochem. Other chemicals were obtained from Sigma.

*Mouse Primary Osteoblast and Chondrocyte Cultures*—All animal experiments were performed according to the guidelines of the International Association for the Study of Pain (25). In addition, the experimental work was reviewed by the committee of Tokyo University charged with confirming ethics. Calvariae dissected from 1–4-day-old mice were washed in phosphate-buffered saline (PBS) and digested with 1 ml of trypsin/EDTA (Invitrogen) containing 10 mg of collagenase (Sigma; type 7) for 10 min × 5 times, and cells from fractions 3–5 were pooled. Cells were plated in 6-multiwell dishes at a density of 5,000 cells/cm$^2$ and grown to confluence in αMEM containing 10% FBS. Chondrocytes were isolated from the ventral parts of the rib cages of 2-day-old mice digested with collagenase D as described previously (26). Cells were plated in 6-multiwell dishes at a density of 5,000 cells/cm$^2$ and grown to confluence in Dulbecco's modified Eagle's medium containing 10% FBS.

*MC3T3-E1 and ATDC5 Cell Cultures*—Mouse osteoblastic MC3T3-E1 cells were maintained and subcultured for 3 or 4 days at 37 °C in a humidified atmosphere of 95% room air:5% $CO_2$ in αMEM containing 10% FBS, 50 units/ml penicillin, 50 mg/ml streptomycin, and 0.2 mM L-ascorbic acid phosphate ester sodium salt in a humidified $CO_2$ incubator. Mouse prechondrocytic ATDC5 cells were obtained from Riken Cell Bank (Saitama, Japan). The cells were grown in a medium consisting of a 1:1 mixture of Dulbecco's modified Eagle's medium and Ham's F-12 medium containing 5% FBS, 10 μg/ml bovine insulin, 10 μg/ml transferin, 3 × $10^{-8}$ M sodium selenite (Roche Molecular Biochemicals), and antibiotics in a humidified $CO_2$ incubator.

*[$^3$H]Thymidine Incorporation*—Mouse primary osteoblastic cells, MC3T3-E1 cells, mouse primary chondrocytes, or ATDC5 cells were inoculated at a density of 5 × $10^4$ cells/well in 24-multiwell plates and cultured to confluence in αMEM or Dulbecco's modified Eagle's medium with 10% FBS for 2 days. The medium was deprived of serum for 12 h before the addition of experimental medium with or without FGFs (FGF-18 at $10^{-12}$ to $10^{-8}$ M, FGF-2 at $10^{-9}$ M, and FGF-10 at $10^{-9}$ M), heparin (2 μg/ml), PD98059 (1, 3, 10, and 30 μM), and SB203580 (1, 3, and 10 μM). [$^3$H]Thymidine (1 μCi/ml in the medium) incorporated for the final 2 h was measured at 18 h.

*Alkaline Phosphatase and Alizarin Red Stainings*—For alkaline phosphatase staining, primary osteoblasts or MC3T3-E1 cells were inoculated at a density of $10^5$ cells/well in 12-multiwell plates and cultured in αMEM containing 10% FBS and 50 μg/ml ascorbic acid with or without FGFs or BMP-2 (300 ng/ml). After 14 days of culture, the cells were fixed with 3.7% (v/v) formaldehyde in PBS and stained for alkaline phosphatase using naphthol AS-MX phosphate (Sigma) in *N,N*-dimethyl formamide as the substrate and Fast BB salt (Sigma) as coupler. For matrix nodule formation, these cells were inoculated at a density of $10^5$ cells/well in 12-multiwell plates and cultured in αMEM containing 10% FBS, 50 μg/ml ascorbic acid, 10 nM dexamethasone, and 10 mM β-glycerophosphate with or without FGFs or BMP-2 for 21 days. The cells were fixed with 3.7% formaldehyde in PBS and stained for Alizarin red at pH 4.0.

*Alcian Blue Staining*—Primary chondrocytes or ATDC5 cells were inoculated at a density of $10^5$ cells/well in 12-multiwell plates and cultured in the medium described above with or without FGFs or BMP-2 (300 ng/ml). After 21 days of culture, the cells were fixed with 3.7% formaldehyde in PBS, stained for 0.1% Alcian blue (Wako Pure Chemicals Co.) in 0.1 N HCl overnight, and rinsed with distilled water. For quantitative analyses, the amount of extractable dye was measured. Alcian blue-stained cultures were extracted with 1 ml of 6 M guanidine-HCl for 6 h at room temperature. The optical density of the extracted dye was measured at a wavelength of 630 nm with a microplate reader (MTP-300; Corona Electric Co.).

*Western Blot Analysis for Tyrosine Phosphorylation of Cellular Proteins*—Mouse primary osteoblasts and chondrocytes and MC3T3-E1 and ATDC5 cells were incubated in αMEM/0.5% FBS for 24 h before treatment with FGF-18 (5 × $10^{-9}$ M) for various periods (0–30 min) and lysed with TNE buffer (10 mM Tris-HCl, 150 mM NaCl, 1% Nonidet P-40, 1 mM EDTA, 10 mM NaF, 2 mM $Na_3VO_4$, 1 mM aminoethylbenzenesulfonyl fluoride, and 10 μg/ml aprotinin). The protein concentration in the cell lysate was measured using a Protein Assay Kit II (Bio-Rad). Equivalent amounts (30 μg) of cell lysates were electrophoresed by 8% SDS-PAGE and transferred to nitrocellulose membrane. After blocking with 5% bovine serum albumin, the membrane was incubated with monoclonal mouse antibody against phosphotyrosine and with peroxidase-conjugated anti-mouse IgG antibody. Phosphotyrosine-containing proteins were visualized using the ECL chemiluminescence reaction (Amersham Biosciences, Inc.) following the manufacturer's instructions. After the antibody was stripped from the membrane, to block nonspecific binding, membranes were incubated with 5% bovine serum albumin and then incubated with monoclonal mouse antibodies against phospho-ERK and phospho-JNK and polyclonal rabbit antibodies against phospho-p38 MAPK, and the immunoreactive bands were visualized as described above.

*Tartrate-resistant Acid Phosphatase-positive Multinucleated Osteoclast Formation in the Coculture of Mouse Primary Osteoblasts and Bone Marrow Cells*—Mouse calvarial primary osteoblasts described above (2 × $10^4$ cells/well) and bone marrow cells prepared from 8-week-old mice (1 × $10^6$ cells/well) were cocultured in 24-multiwell dishes containing αMEM/10% FBS with or without FGFs for 6 days with a medium change at 3 days. After 6 days of culture, the cells were fixed with 3.7% formaldehyde in PBS and ethanol-acetone (50:50, v/v) and stained at pH 5.0 in the presence of L(+)-tartaric acid using naphthol AS-MX phosphate in *N,N*-dimethyl formamide as the substrate. Tartrate-resistant acid phosphatase-positive-multinucleated cells containing more than three nuclei were counted as osteoclasts.

*Resorbed Pit Formation Assay in the Coculture of Mouse Primary Osteoblasts and Bone Marrow Cells*—Mouse osteoblasts (1 × $10^6$ cells/dish) and bone marrow cells (2 × $10^7$ cells/dish) prepared as described above were cocultured on 10-cm culture dishes coated with 0.24% collagen gel matrix (Nitta Gelatin, Tokyo, Japan) containing αMEM with 10% FBS, 1,25$(OH)_2$ vitamin $D_3$ ($10^{-8}$ M), and prostaglandin $E_2$ ($10^{-6}$ M) for 6 days, with a medium change every 3 days, and for 1 additional day in αMEM/10% FBS without bone-resorbing factors. After 7 days of culture, nonadherent cells were washed with PBS, and adherent cells were stripped by 0.2% bacterial collagenase. An aliquot of crude osteoclast preparation (0.1 ml) was further cultured on a dentine slice placed in each well of 96-well dishes containing αMEM/10% FBS in the presence or absence of FGFs. After 24 h of culture, cells were removed with 1 N $NH_4OH$ solution, and stained with 0.5% toluidine blue. Total area was estimated under a light microscope with a micrometer to assess osteoclastic bone resorption using an image analyzer (System Supply Co., Nagano, Japan). At the same time, cells on a dentine slice in the independent culture were fixed with 3.7% (v/v) formaldehyde in PBS and ethanol-acetone (50:50, v/v), and stained at pH 5.0 in the presence of L(+)-tartaric acid using naphthol AS-MX phosphate (Sigma) in *N,N*-dimethyl formamide as substrate. Tartrate-resistant acid phosphatase-positive multinucleated cells containing more than three nuclei were counted as osteoclasts.

*Statistical Analysis*—Means of groups were compared by analysis of variance, and the significance of differences was determined by *post hoc* testing using Bonferroni's method.

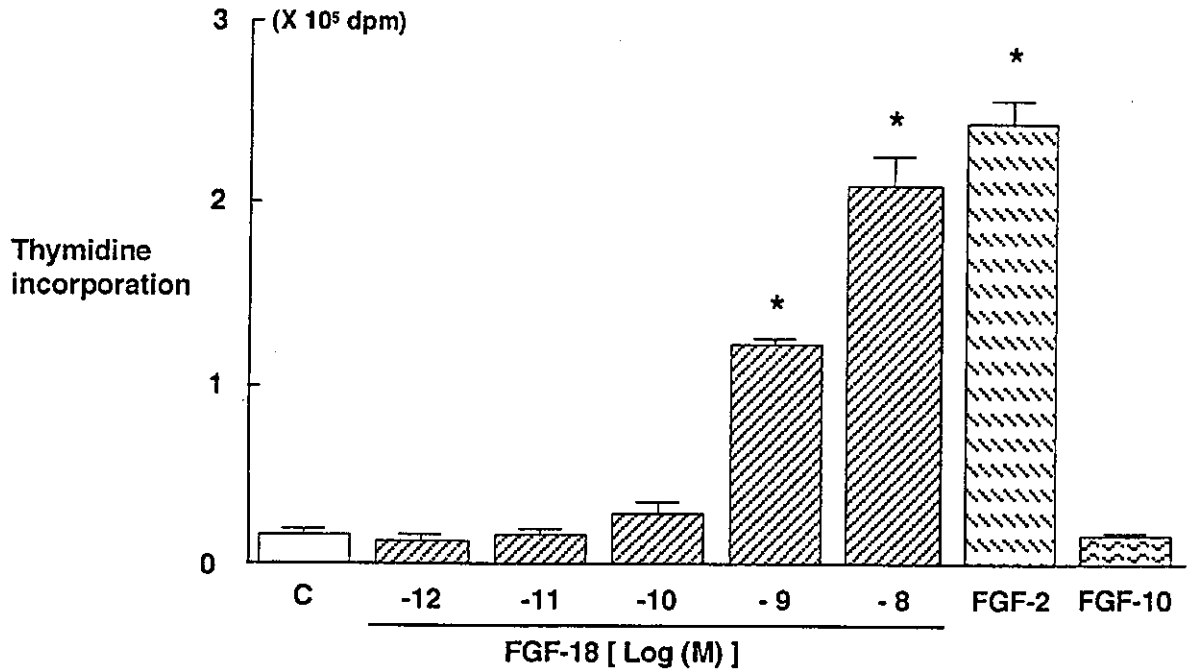


FIG. 1. **Effect of FGF-18 on proliferation of osteoblasts.** Mouse primary osteoblasts were cultured with or without FGF-18 ($10^{-12}$ to $10^{-8}$ M), FGF-2 ($10^{-8}$ M), or FGF-10 ($10^{-8}$ M) for 16 h, and cell proliferation was determined by [$^3$H]thymidine incorporation into DNA. Data are expressed as means (*bars*) ± S.D. (*error bars*) for 8 wells/group. *, $p < 0.01$, significant stimulation by FGFs.

RESULTS

*Effects of FGF-18 on Functions of Osteoblasts*—Effects of FGF-18 ($10^{-12}$ to $10^{-8}$ M), FGF-2 ($10^{-8}$ M), and FGF-10 ($10^{-8}$ M) on the proliferation of primary osteoblasts were determined by [$^3$H]thymidine incorporation into DNA (Fig. 1). FGF-18 ($\geq 10^{-9}$ M) dose-dependently stimulated cell proliferation up to approximately10-fold of control cultures. Although heparan sulfate or heparin is reported to modulate the mitogenic activity of several FGFs (27, 34), the mitogenic effect of FGF-18 was not altered by adding heparin to the culture (data not shown). This mitogenic action was similar to those of FGF-2, whereas FGF-10 did not affect cell proliferation. All of these results were reproducible in the culture of mouse osteoblastic MC3T3-E1 cells (data not shown).

To further study the effects of FGFs on differentiation and matrix synthesis of osteoblasts, cultured primary osteoblasts were stained with alkaline phosphatase, a marker for osteoblast differentiation, at 14 days and with Alizarin red, a marker for matrix synthesis, at 21 days, respectively (Fig. 2). FGF-18 dose-dependently decreased both stainings in both cell culture systems. These inhibitory actions on differentiation and matrix synthesis were similarly seen in FGF-2-treated cultures, whereas FGF-10 affected none of these stainings. BMP-2, a positive control, potently stimulated both stainings. The effects of these growth factors were similarly seen in the MC3T3-E1 cell culture (data not shown).

*Signal Transduction of FGF-18 in Osteoblasts*—Fig. 3*A* shows the time course of effects of FGF-18 on tyrosine phosphorylation of cellular proteins in the primary osteoblast culture. Several proteins were selectively phosphorylated by FGF-18 ($10^{-9}$ M) at a time as early as 2 min. Western blot analyses using antibodies against specific proteins related to MAPKs revealed that phosphorylation of ERK was induced by FGF-18 at 2 min and was maintained for 30 min, although neither p38 nor JNK MAPK phosphorylation was affected for 30 min (Fig. 3*A*). To examine the functional relevance of the activation of MAPKs by FGF-18 in osteoblasts, PD98059, a

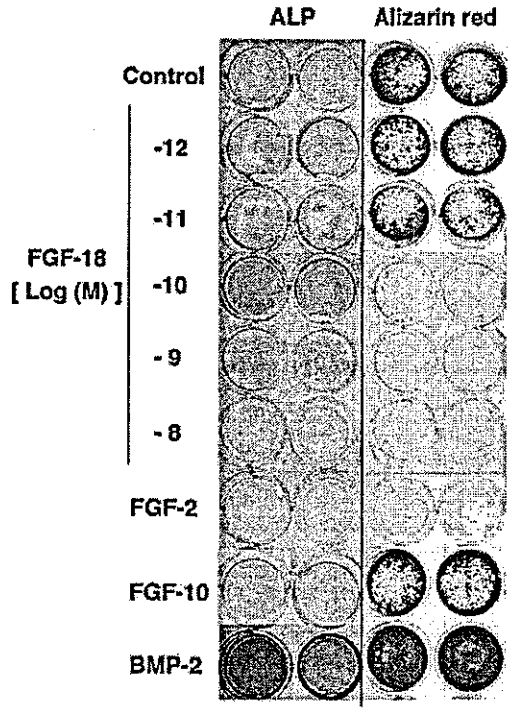


FIG. 2. **Effect of FGF-18 on differentiation and matrix synthesis of osteoblasts.** Mouse primary osteoblasts were cultured with or without FGF-18 ($10^{-12}$ to $10^{-8}$ M), FGF-2 ($10^{-8}$ M), FGF-10 ($10^{-8}$ M), or BMP-2 (300 ng/ml). Alkaline phosphatase and Alizarin red stainings were performed after 14 and 21 days of culture, respectively.

specific inhibitor of the upstream kinase of ERK (28), and SB203580, a specific inhibitor of p38 MAPK (29), were added to the primary osteoblast culture. PD98059 and SB203580 were confirmed to show specific inhibition of the phosphorylation of

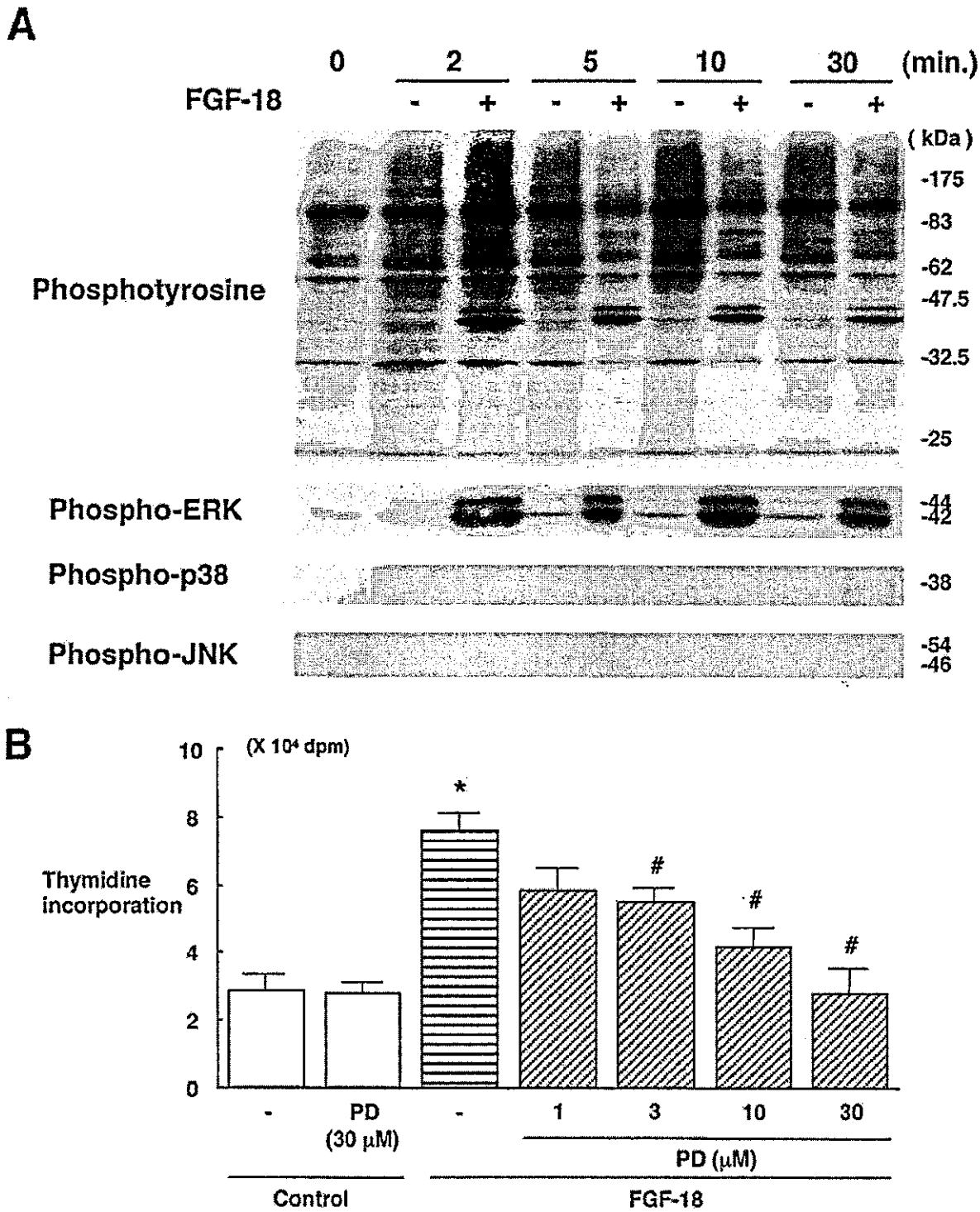


FIG. 3. **Intracellular signaling of FGF-18 in osteoblasts.** *A*, effect of FGF-18 on phosphorylation of cellular proteins and MAPKs in primary osteoblasts. Mouse primary osteoblasts were cultured with and without FGF-18 ($10^{-9}$ M) for various time periods (2–30 min) and lysed with TNE buffer. Cell lysates (20 $\mu$g) were subjected to 8% SDS-PAGE and immunoblotted with polyclonal antibodies against phosphotyrosine, phospho-ERK, phospho-p38 MAPK, and phospho-JNK as described under "Experimental Procedures." *B*, effect of PD98059 (*PD*) on FGF-18-stimulated [$^3$H]thymidine incorporation into primary osteoblasts. Mouse primary osteoblasts were cultured with and without FGF-18 ($10^{-9}$ M) and PD98059 (1, 3, 10, and 30 $\mu$M). After 16 h of culture, cell proliferation was determined by [$^3$H]thymidine incorporation into DNA. Data are expressed as means (*bars*) ± S.D. (*error bars*) for 8 wells/group. *, $p < 0.01$, significant stimulation by FGF-18; #, $p < 0.01$, significant inhibition by PD98059.

ERK and p38 MAPK, respectively, in both the presence and absence of FGF-18 by Western blot analyses (data not shown). PD98059 dose-dependently inhibited the stimulation of FGF-18 on [$^3$H]thymidine incorporation to the levels of the control culture (Fig. 3*B*), whereas SB203580 (up to the maximum concentration of 10 $\mu$M) did not affect FGF-18 stimulation

TABLE I
*Effects of FGFs on proliferation and differentiation of cultured primary chondrocytes*
Data are expressed as means ± S.D. for 8 wells/group.

| | Thymidine incorporation | Alcian blue |
|---|---|---|
| | $\times 10^4$ *dpm* | $\times 10^{-1}$ *OD* |
| Control | 3.53 ± 0.27 | 4.09 ± 0.11 |
| FGF-18 | | |
| $10^{-12}$ M | 3.74 ± 0.47 | 3.80 ± 0.04 |
| $10^{-11}$ M | 5.94 ± 1.07 | 3.85 ± 0.13 |
| $10^{-10}$ M | 23.00 ± 3.17[a] | 3.74 ± 0.11 |
| $10^{-9}$ M | 25.06 ± 2.67[a] | 2.72 ± 0.11[a] |
| $10^{-8}$ M | 28.05 ± 4.71[a] | 1.97 ± 0.12[a] |
| FGF-2 ($10^{-8}$ M) | 32.08 ± 3.08[a] | 1.96 ± 0.08[a] |
| FGF-10 ($10^{-8}$ M) | 3.67 ± 0.34 | 4.00 ± 0.13 |
| BMP-2 (300 ng/ml) | | 5.54 ± 0.19[a] |

[a] $p < 0.01$, significantly different from control.

(data not shown). Similar results were seen when MC3T3-E1 cells were used instead of primary osteoblasts (data not shown). These results suggest that the ERK pathway functionally contributes to the FGF-18 mitogenic action on osteoblasts.

*Effects of FGF-18 on Functions of Chondrocytes*—Similar to the investigation on osteoblasts, the effects of FGF-18, FGF-2, and FGF-10 on chondrocyte proliferation were examined by [$^3$H]thymidine incorporation into cultured primary chondrocytes (Table I). FGF-18 ($\geq 10^{-10}$ M) stimulated cell proliferation in the cultures. These effects also did not differ in the presence or absence of heparin (data not shown). These mitogenic effects were similar to those of FGF-2, whereas FGF-10 did not affect these cells. To study the effects of FGFs on differentiation/matrix synthesis of chondrocytes, accumulation of sulfated glycosaminoglycan in cultured primary chondrocytes was determined by Alcian blue staining (Table I). FGF-18 ($\geq 10^{-9}$ M) decreased the intensity of Alcian blue staining, whereas BMP-2 significantly stimulated it. This inhibitory action on chondrocyte differentiation was also seen in FGF-2-treated cultures, but not in FGF-10-treated cultures. These results were reproducible when mouse prechondrocytic ATDC5 cells were used instead of primary chondrocytes (data not shown).

*Signal Transduction of FGF-18 in Chondrocytes*—Immunoblot analysis using an anti-phosphotyrosine antibody revealed that several intracellular proteins were phosphorylated by FGF-18 ($10^{-9}$ M) at a time as early as 2 min in cultured primary chondrocytes (Fig. 4*A*). Among MAPKs, FGF-18 induced not only phosphorylation of ERK but also that of p38 MAPK at 2–5 min, although JNK MAPK was hardly phosphorylated for 30 min. Both PD98059 and SB203580, whose specific inhibitions of phosphorylation were also confirmed by Western blottings in this culture system, dose-dependently inhibited the stimulation of FGF-18 on [$^3$H]thymidine incorporation to the levels of the control culture (Fig. 4*B*). This result indicates the involvement of the activation of ERK and p38 MAPK in chondrocyte proliferation by FGF-18. Similar results were seen when the ATDC5 cell culture system was used (data not shown).

*Effects of FGF-18 on Osteoclast Formation and Function*—To study the effects of FGF-18 on bone resorption, tartrate-resistant acid phosphatase-positive multinucleated osteoclast formation in the coculture system of mouse primary osteoblasts and bone marrow cells was examined. FGF-18 ($\geq 10^{-10}$ M) dose-dependently stimulated osteoclast formation (Table II). This induction was similar to that of FGF-2, whereas FGF-10 did not affect it. Because we reported previously that FGF-2 stimulated osteoclast formation through induction of cyclooxygenase-2 and RANKL (13–15, 17), we added NS-398 ($10^{-6}$ M), a specific inhibitor of cyclooxygenase-2, and osteoprotegerin (10 ng/ml), a soluble decoy receptor of RANKL. The stimulation of osteoclastogenesis by FGF-18 was decreased ~80% by NS-398 and almost completely abolished by osteoprotegerin. Hence, like FGF-2, FGF-18 stimulation of osteoclastogenesis was shown to be mediated by both cyclooxygenase-2 and RANKL.

To determine the direct action of FGF-18 on mature osteoclast function, the pit area on a dentine slice resorbed by osteoclasts formed in the coculture of mouse osteoblasts and bone marrow cells was measured. FGF-18 ($\geq 10^{-9}$ M) dose-dependently stimulated the resorbed pit area up to 5.7-fold of the control culture (Table III). This stimulation was not due to the increase in the number of osteoclasts but rather to the activation of each osteoclast function because the number of tartrate-resistant acid phosphatase-positive multinucleated osteoclasts on a dentine when the resorbed pit area was measured was not affected by FGF-18 (Table III). In fact, the effect of FGF-18 on the pit area per osteoclast (resorbed pit area/osteoclast number in a dentine slice) showed a pattern similar to that seen on the resorbed pit area (Table III). This stimulatory action of FGF-18 on mature osteoclast function was reproducible in the culture system of osteoclasts that were isolated from neonatal rabbit long bones with higher purity (30) (data not shown). These results suggest that FGF-18 directly stimulates mature osteoclast function as seen in FGF-2, but not in FGF-10.

## DISCUSSION

This study demonstrated that FGF-18, a novel member of the FGF family, stimulated the proliferation of osteoblasts through ERK activation and stimulated that of chondrocytes through ERK and p38 MAPK activation. FGF-18, however, showed inhibitory actions on the differentiation and matrix synthesis of both kinds of cells. With regard to the effect on osteoclasts, FGF-18 stimulated osteoclast formation through cyclooxygenase-2 and RANKL. It also exhibited a stimulatory action on osteoclasts to resorb bone. All of these findings were similar to those of FGF-2, as shown in our present and previous studies (10, 11, 13, 15–17). FGF-10, on the other hand, did not show any regulation on these bone and cartilage cells.

The FGFR family consists of four distinct tyrosine kinase receptors and several isoforms of these receptors that are generated by alternative RNA splicing (1, 2). The main difference between FGF-18 and FGF-2 is their specificities to receptors: FGF-18 activates FGFR3c strongly and FGFR2c weakly but does not activate other receptors, whereas FGF-2 can activate all FGFRs (FGFR1 to FGFR4) (31, 32). FGF-2 is recognized as a potent mitogen for a variety of mesenchymal cells (32). FGF-18 is also reported to activate cell proliferation of cultured NIH 3T3 fibroblastic cells; however, this activity was much lower than that of FGF-2 (23, 24). In the present study, the mitogenic actions of FGF-18 on osteoblasts and chondrocytes were as strong as those of FGF-2, suggesting that FGF-18 is more specific to bone and cartilage cells than FGF-2. Furthermore, *Fgf-2*-deficient mice showed mild abnormalities in bone and cartilage development (12), whereas *Fgf-18*-deficient mice exhibited severe developmental retardation of calvariae and long bones.[2] From these results, it is speculated that FGF-18 can almost fully compensate for the role of FGF-2, although FGF-2 cannot replace FGF-18, for bone and cartilage formation. We further propose that the signalings through FGFR3c and FGFR2c might be important for the regulation of bone and cartilage formation.

The mechanism by which FGFs stimulate cell proliferation is thought to be mediated by heparan sulfate proteoglycans at the cell surface (33, 34). Heparan sulfate is the most structurally complex glycosaminoglycan made by animal cells and is chemically related to heparin but markedly different from it in

[2] N. Ohbayashi and N. Itoh, unpublished observation.

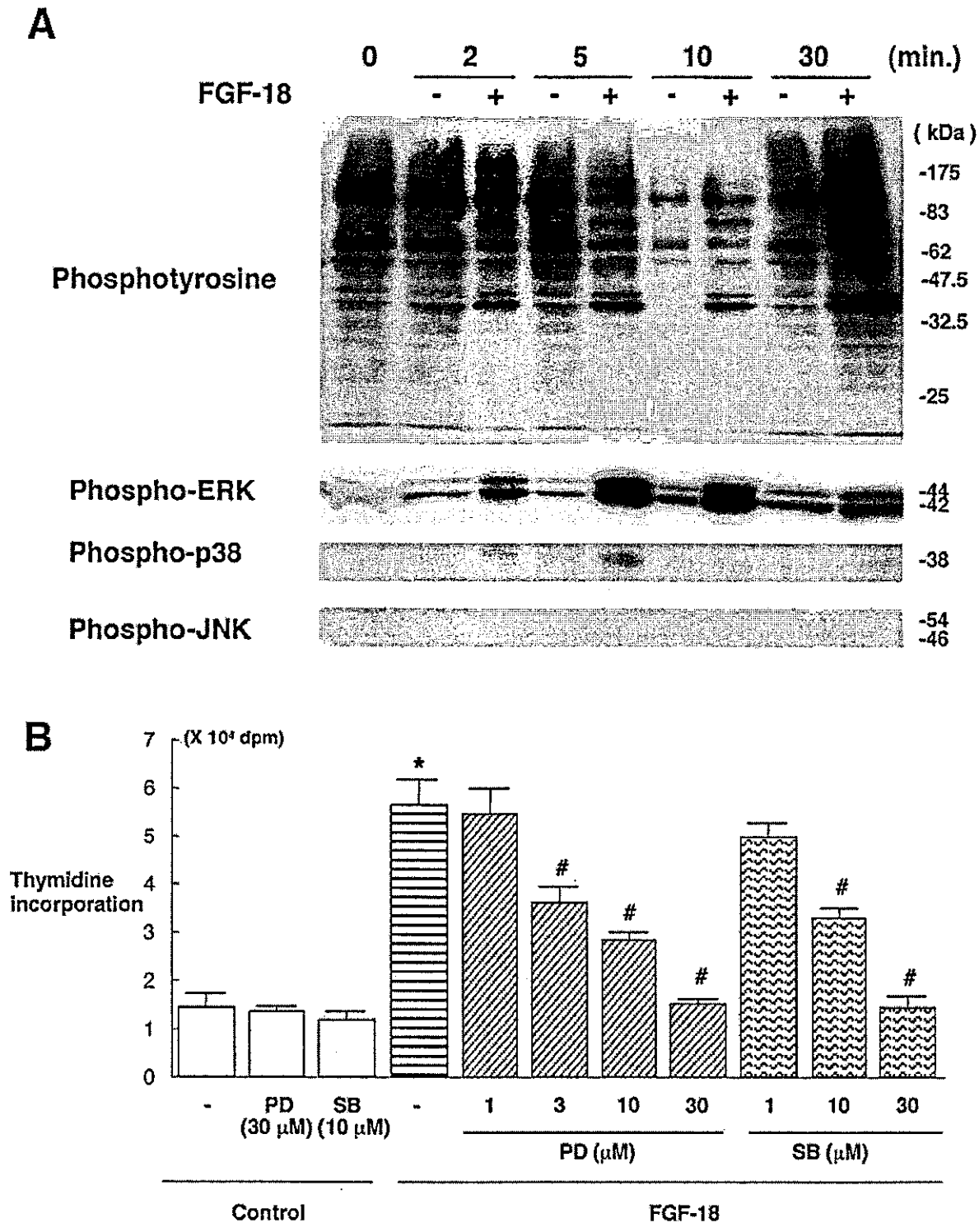


FIG. 4. **Intracellular signaling of FGF-18 in chondrocytes.** *A*, effect of FGF-18 on phosphorylation of cellular proteins and MAPKs in primary chondrocytes. Mouse primary chondrocytes were cultured with and without FGF-18 ($10^{-9}$ M) for the indicated time periods (2–30 min) and lysed with TNE buffer. Immunoblottings with polyclonal antibodies against phosphotyrosine, phospho-ERK, phospho-p38 MAPK, and phospho-JNK were performed as described under "Experimental Procedures." *B*, effects of PD98059 (*PD*) and SB203580 (*SB*) on FGF-18-stimulated [$^3$H]thymidine incorporation into primary chondrocytes. Mouse primary chondrocytes were cultured with and without FGF-18 ($10^{-9}$ M), PD98059 (1, 3, 10, and 30 μM), and SB203580 (1, 3, and 10 μM). After 16 h of culture, cell proliferation was determined by [$^3$H]thymidine incorporation into DNA. Data are expressed as means (*bars*) ± S.D. (*error bars*) for 8 wells/group. *, $p < 0.01$, significant stimulation by FGF-18; #, $p < 0.01$, significant inhibition by PD98059 or SB203580.